

OPEN-FILE REPORT 12-01

Antero Reservoir Quadrangle Geologic Map, Park and Chaffee Counties, Colorado

Authors' Notes

**Includes Description of Map Units, Stratigraphy, Structural Geology,
Mineral Resources, Water Resources, and Geologic Hazards,**



John W. Hickenlooper, Governor
State of Colorado



Mike King, Executive Director
Department of Natural Resources



Vincent Matthews
State Geologist and Director
Colorado Geological Survey

by

Robert M. Kirkham, Karen J. Houck, Christopher J. Carroll, and Alyssa D. Heberton-Morimoto

Colorado Geological Survey
Department of Natural Resources
Denver, Colorado
2012

Antero Reservoir Quadrangle Geologic Map, Park and Chaffee Counties, Colorado



View to northeast across the Pinedale outwash terrace of Salt Creek towards Antero Reservoir. Rolling topography and closed depressions on the terrace is karst topography formed by dissolution of evaporite in the Minturn Formation. Photograph taken from back porch of historic cabin at Salt Works ranch [UTMX: 417830, UTM Y: 4312281]. Three dark objects along fence in right side of photograph are remnants of copper boilers used to produce halite from the 1860s to the 1880s.

by

Robert M. Kirkham¹, Karen J. Houck², Christopher J. Carroll³, and Alyssa D. Heberton-Morimoto³

¹ GeoLogical Solutions, Alamosa, CO

² Dinosaur Tracks Museum, University of Colorado Denver, Denver, CO

³ Colorado Geological Survey, Denver, CO

This mapping project was funded jointly by the Colorado Geological Survey
and the U.S. Geological Survey through the National Geologic
Mapping Program under STATEMAP Agreement No. 07HQAG0083

FOREWORD

The purpose of the Colorado Geological Survey's (CGS) *Antero Reservoir Quadrangle Geologic Map, Park and Chaffee Counties, Colorado* is to describe the geology, mineral and ground-water resources, and geologic hazards of this 7.5-minute quadrangle located in central Colorado. Consulting geologists Robert Kirkham and Karen Houck, CGS staff geologist Chris Carroll, and field assistant Alyssa Heberton-Morimoto completed field work for the project during the 2007 field season. Mr. Kirkham, Dr. Houck, and Mr. Carroll, the principal mappers and authors, created this report using field maps, photographs, structural measurements, and field notes generated by all four investigators.

This mapping project was funded jointly by the U.S. Geological Survey (USGS) and the CGS. USGS funding comes from the STATEMAP component of the National Cooperative Geologic Mapping Program, award number 07HQAG0083, authorized by the National Geologic Mapping Act of 1997, reauthorized in 2009. CGS matching funding comes from the Colorado Department of Natural Resources Severance Tax Operational Funds, from severance taxes paid on the production of natural gas, oil, coal, and metals in Colorado.

Vince Matthews
State Geologist and Director
Colorado Geological Survey

TABLE OF CONTENTS

	page
FOREWORD.....	v
TABLE OF CONTENTS.....	vi
LIST OF FIGURES.....	vi
LIST OF TABLES.....	vii
LIST OF PLATES.....	vii
LIST OF APPENDICES.....	vii
INTRODUCTION.....	1
DESCRIPTION OF MAP UNITS.....	6
SURFICIAL DEPOSITS.....	6
BEDROCK UNITS.....	11
STRATIGRAPHY.....	30
STRUCTURAL GEOLOGY.....	34
MINERAL RESOURCES.....	38
WATER RESOURCES.....	41
GEOLOGIC HAZARDS.....	43
ACKNOWLEDGMENTS.....	45
REFERENCES CITED.....	46

LIST OF FIGURES

Figure 1. Shaded relief map of the project area and adjoining areas.....	1
Figure 2. Location map and status of geologic mapping in adjacent areas.....	2
Figure 3. Geologic time scale.....	4
Figure 4. Exposure of unit Qa2 in an inactive gravel pit.....	7
Figure 5. Hills underlain by Wagontongue Formation rise up from Antero Formation strike valley.....	11
Figure 6. Limestone beds in the Antero Formation.....	13
Figure 7. Total alkali-silica diagram of volcanic and selected intrusive rock samples.....	15
Figure 8. Tertiary limestone unit composed sparry limestone or calcareous tufa.....	16
Figure 9. Conglomeratic facies of the Tallahassee Creek Conglomerate.....	19
Figure 10. Plant fossils in the upper member of the Minturn Formation.....	23
Figure 11. Limestone bed in the upper member of the Minturn Formation.....	24
Figure 12. Vuggy limestone in the evaporite facies of the Minturn Formation.....	24

Figure 13. Overview of buttes, hills, and peaks capped by Eocene volcanic rocks.....	37
Figure 14. Historical photograph of the Salt Works Ranch	39
Figure 15. Prospect pit or small mine in an outcrop of contorted gypsum.....	39
Figure 16. Cluster of sinkholes and karst topography on the valley floor of Salt Creek.....	43

LIST OF TABLES

Table 1. $^{40}\text{Ar}/^{39}\text{Ar}$ ages of igneous rocks.....	12
---	----

LIST OF PLATES

Plate 1. Antero Reservoir quadrangle geologic map
Plate 2. Correlation of map units, 3-D map, and cross section

LIST OF APPENDICES

Appendix A. Whole-rock major-element geochemical analyses.....	50
Appendix B. $^{40}\text{Ar}/^{39}\text{Ar}$ geochronology results from the Antero Reservoir quadrangle.....	51

INTRODUCTION

The Antero Reservoir 7.5-minute quadrangle lies in the southwestern part of South Park, a high-altitude intermontane valley in central Colorado. The map area covers approximately 57 square miles in Park and Chaffee Counties (Fig. 1). U.S. Highways 285 and 24 cross the quadrangle.

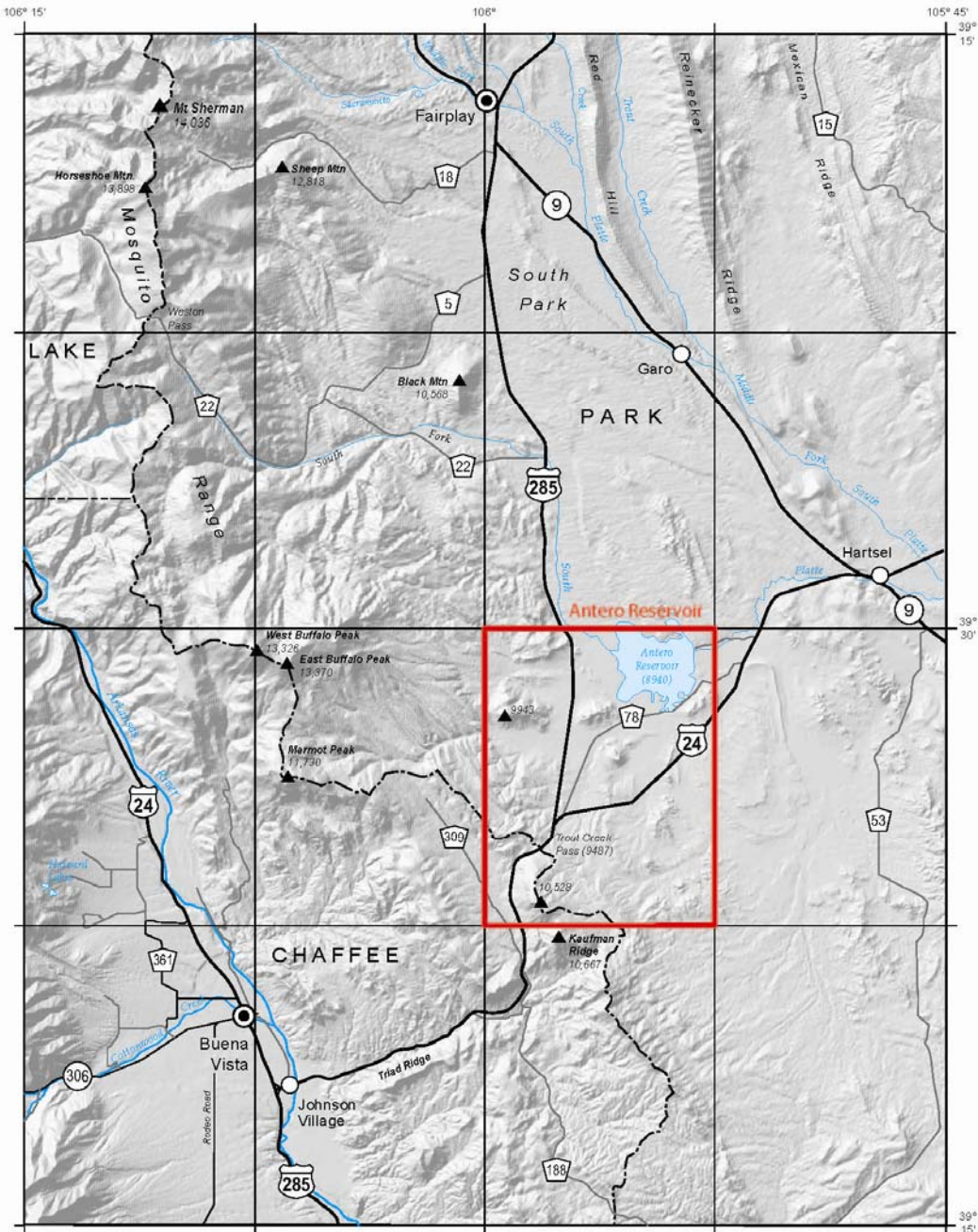


Figure 1. Shaded relief map of the project area and adjoining areas. The thick red line outlines the Antero Reservoir quadrangle.

The Colorado Geological Survey (CGS) mapped the geology of the Antero Reservoir quadrangle as part of the STATEMAP component of the National Cooperative Geologic Mapping Program. This geologic map is one of several recently completed geologic maps in this region that the CGS prepared as part of the STATEMAP program (Fig. 2). Mr. Kirkham mapped the Tertiary bedrock and the Quaternary surficial deposits. Ms. Houck, Mr. Carroll, and Ms. Heberton-Morimoto mapped the Paleozoic and Precambrian rocks.

Field work was conducted during the summer and fall of 2007. Geologic information and ground control collected in the field were plotted on 1:24,000-scale color aerial photographs flown for the U.S. Forest Service in 1997. The annotated aerial photographs were scanned, geo-referenced, and imported into ERDAS Imagine OrthoBase, where they were photogrammetrically corrected and rendered in 3D. Line work was traced directly from stereo pair images of the aerial photographs in ERDAS Imagine Stereo Analyst and exported as ESRI shapefiles into ArcGIS.

Numerous previously published geologic maps and reports address all or parts of the Antero Reservoir quadrangle. These include the regional 1:500,000-scale geologic maps of Colorado by Tweto (1979), the 1:250,000-scale geologic map of the Pueblo 1° x 2° quadrangle by Scott and others (1978), and the 1:125,000-scale geologic map of Stark and others (1949). More detailed mapping that was useful to our investigation include the 1:48,000-scale map of De Voto (1971), as well as the unpublished reconnaissance map by Scott (2008), which utilizes field work from 1971 and 1972. The CGS recently published several 1:24,000-scale geologic maps of areas adjacent to or near the Antero Reservoir quadrangle (Fig. 2).

Figure 3 shows the divisions of geologic time and the age estimates of their boundaries. Grain-size terminology for sedimentary deposits (both bedrock and surficial deposits) follows the modified Wentworth grain-size scale (Ingram, 1989). This classification system defines three basic size clasts on the basis of grain-size diameter: gravel is larger than 0.08 inches in diameter (2 mm), sand is 0.08 to 0.0024 inches in diameter (2 to 0.062 mm), and mud is smaller than 0.0024 inches in diameter (0.062 mm). Pebbles, cobbles, and boulders are differing sizes of gravel; sand sizes ranges from very fine to very coarse; and mud is divided into clay and silt sizes. The terms pebbles, cobbles, and boulders are commonly used by many geologists for large diameter rounded grains deposited in fluvial and beach environments (for example, Jackson, 1997); however, we use these terms only to describe the size of the gravel, not its origin.

The term “clast” refers to rock and mineral fragments that are in the gravel size class, whereas matrix refers to surrounding material that is in the sand and mud sizes. In clast-supported deposits, the majority of the material consists of clasts that are in point-to-point contact. Matrix-supported deposits are composed predominantly of material smaller than 2 mm, and most clasts are separated by or embedded in matrix. Terms used for sediment sorting are those of Folk and Ward (1957). Sedimentary rocks are named according to the classification system of Folk (1980). English units are used throughout the report except for microscopic observations and other small sizes, which are described in metric units. The 1983 North American datum is used for all UTM coordinates.

Selected samples were chemically analyzed for major elements. The analytical results are in Appendix A. Locations of the analyzed samples are shown on the geologic map and are also described in Appendix A. The total alkali-silica plot (TAS) of Le Bas and others (1986) was used to classify chemically analyzed volcanic rocks. Two samples from the quadrangle were dated using $^{40}\text{Ar}/^{39}\text{Ar}$ methods (see Appendix B).

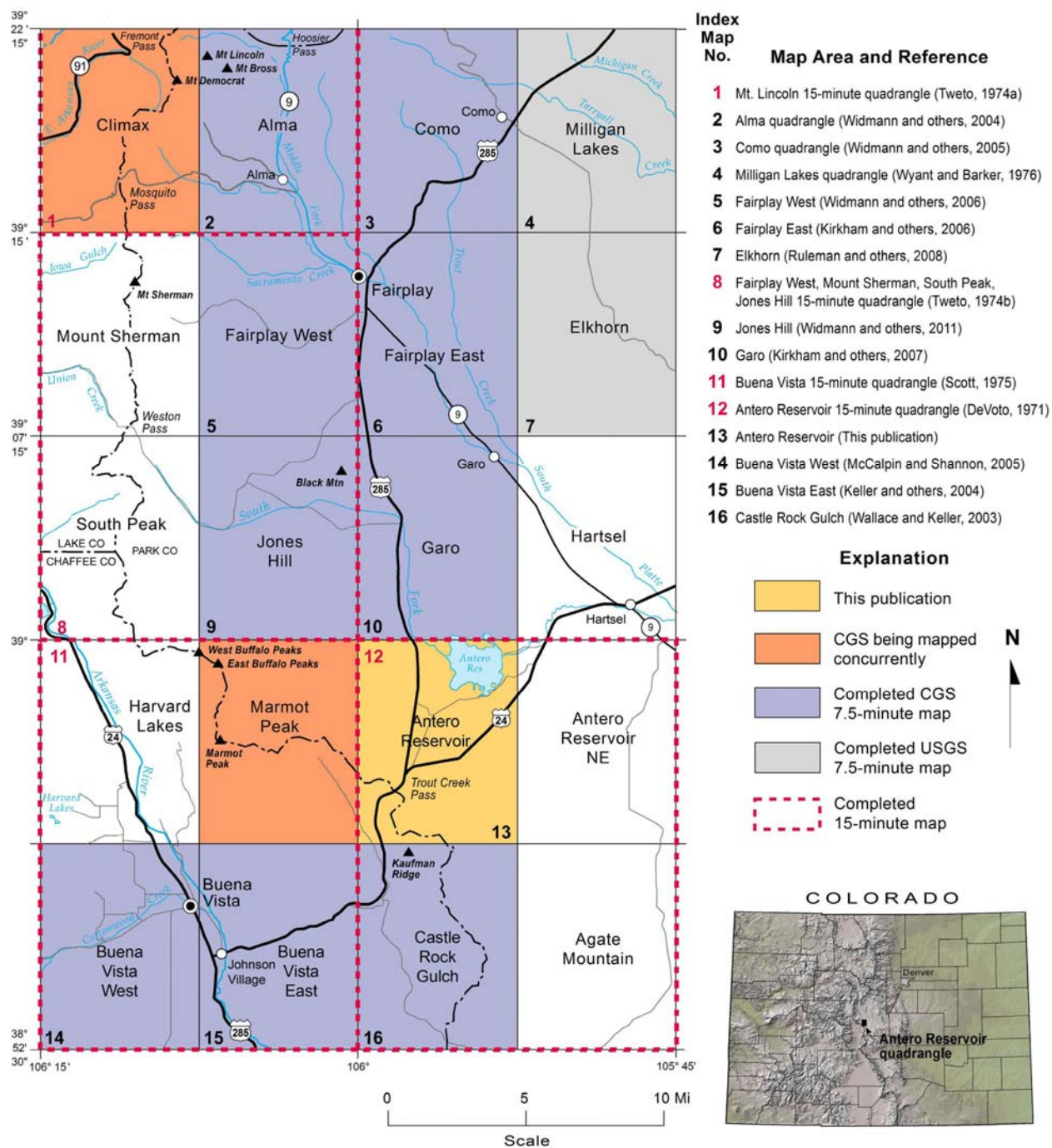


Figure 2. Location map and status of geologic mapping in adjacent areas.

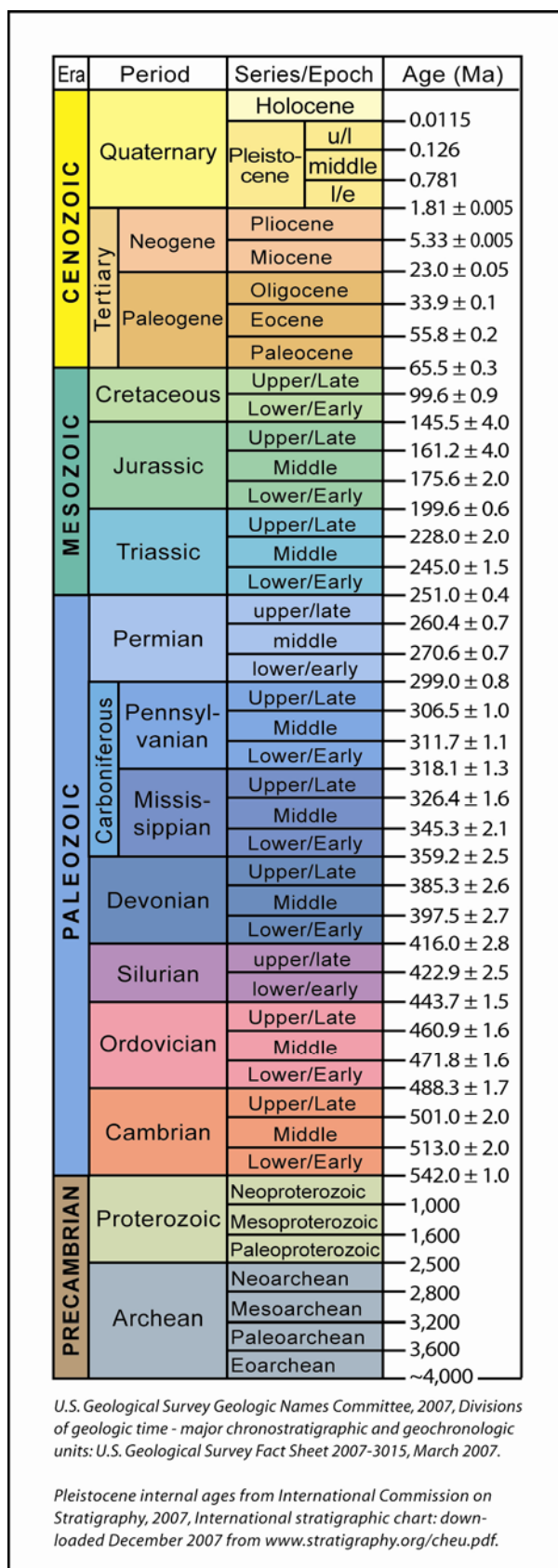


Figure 3. Geologic time scale

Surficial geologic deposits are divided into map units on the basis of either genesis or landform and also relative age. Most of the surficial deposits in the map area are not well exposed. Due to limited exposures, the physical attributes of the surficial units such as thickness, texture, stratification, and composition are described from observations made at only a few locations, and their origin often is deduced only on the basis of geomorphic characteristics.

Generally, surficial deposits with a minimum thickness of about 3 to 5 feet thick are shown on the map. Surficial deposits associated with distinct landforms such as terraces locally may be thinner than 3 feet. Contacts for many surficial units were located using geomorphic characteristics, and some contacts are gradational. Areas mapped as surficial deposits may include small areas of bedrock that are not shown on the map. Deposits of residuum are not mapped. Soil-horizon nomenclature of Birkeland (1999) and Machette (1985) was utilized during the project.

Absolute ages are not available for any of the surficial deposits in the map area. Characteristics such as stratigraphic relations, position in the landscape, degree of weathering, and pedogenic soil development were used to estimate the relative ages of the surficial deposits. Glacial till and outwash deposited by glacial meltwater are correlated with oxygen-isotope stages wherever possible in this report. Oxygen occurs in two common stable isotopes, ^{16}O and ^{18}O . The ratio of these two isotopes in water is temperature dependent. During cold glacial periods the $^{18}\text{O}/^{16}\text{O}$ ratio is high, and during warmer interglacial periods the ratio is low. By studying oxygen isotope ratios in thick ice caps and in fossils buried beneath the sea floor, changes in temperature over time can be evaluated (Martinson and others, 1987). An oxygen-isotope stage consists of a lengthy time interval during which the temperature was generally either cold or warm. The modern warm interglacial period is assigned to oxygen-isotope stage one, the last major glacial period (Pinedale glaciation) is oxygen-isotope stage 2, and preceding interglacial and glacial periods are consecutively numbered. The Bull Lake glaciation is usually correlated with isotope stage 6.

Bedrock outcrops and surficial deposits which are less than about 50 feet wide generally are not depicted on the map. Thin but important bedrock units, such as limestone beds and igneous dikes, are represented on the map as single lines because they add to the stratigraphic and structural understanding of the geology in the area.

DESCRIPTION OF MAP UNITS

SURFICIAL DEPOSITS - Surficial deposits are organized into four groups on the basis of their genesis. The genetic groups are human-made deposits; alluvial deposits; mass-wasting deposits; and alluvial and mass-wasting deposits.

Human-Made Deposits

af Artificial fill (historic) — Unsorted sand, silt, gravel, or rock fragments used as fill for dams, roads, and a now abandoned railroad. Maximum thickness is about 30 feet.

mw Mine waste (historic) — Unsorted sand, gravel, silt, and rock debris in waste piles at inactive or abandoned mines. Maximum thickness is approximately 20 feet.

Alluvial Deposits

Qa1 Alluvial unit one (Holocene) — Mainly poorly sorted, clast-supported, unconsolidated, sandy gravel, gravelly sand, silty sand, and sandy silt in modern channels, flood plains, and adjacent low-lying terraces that are approximately 5 feet or less above modern channels. All sizes of gravel are present. Deposits commonly are stratified and may have cut-and-fill channels. Beds of organic-rich sediment or peat are locally present. Peat and organic-rich silty sediment may be found in topographic depressions associated with karst topography. Most gravel clasts within the unit are fresh and sound. Clasts typically are subround to subangular, although a few are round or angular. Only weakly developed pedogenic soil horizons have formed on deposits of alluvial unit one. The unit probably was deposited as outwash during episodes of Holocene neoglaciation or as hyperconcentrated flood deposits during oxygen isotope stage 1. Maximum thickness of the unit is estimated to be about 10 feet thick in most places but could be thicker locally.

Qa2 Alluvial unit two (late Pleistocene) — Stratified, poorly sorted, clast-supported, sandy cobble and pebble gravel, gravelly sand, silty sand, and sandy silt that was deposited by glacial meltwater. Gravel clasts within the unit commonly are subround to subangular, and they are unweathered or only very slightly weathered. Deposits of alluvial unit two occur in the valleys of the South Fork of the South Platte River, Buffalo Creek, Spring Creek, and Salt Creek. The gravel clasts typically are larger (cobble and pebble sizes) in the deposits in the valley of the South Fork of the South Platte. Pebble-sized clasts are dominant in other valleys. The best exposure of the unit is in a gravel pit near the center of the NE $\frac{1}{4}$ of section 31, T. 12 S., R. 76 W. (Fig. 4).

Streams have incised about 3 to 15 feet below the position of alluvial unit two. Pedogenic soils formed in alluvial unit two have weakly to moderately well developed Bw horizons, absent or very weak and thin argillic Bt horizons, and thin calcareous Bk horizons with carbonate morphology varying from stage I to weak stage III. The amount of pedogenic carbonate is relatively high in some outcrops (Fig. 4). This may be related to a high dissolved calcium content of surface and ground water in those areas. Also, calcium-rich eolian dust derived from the evaporite facies of the Minturn Formation may have accumulated on deposits

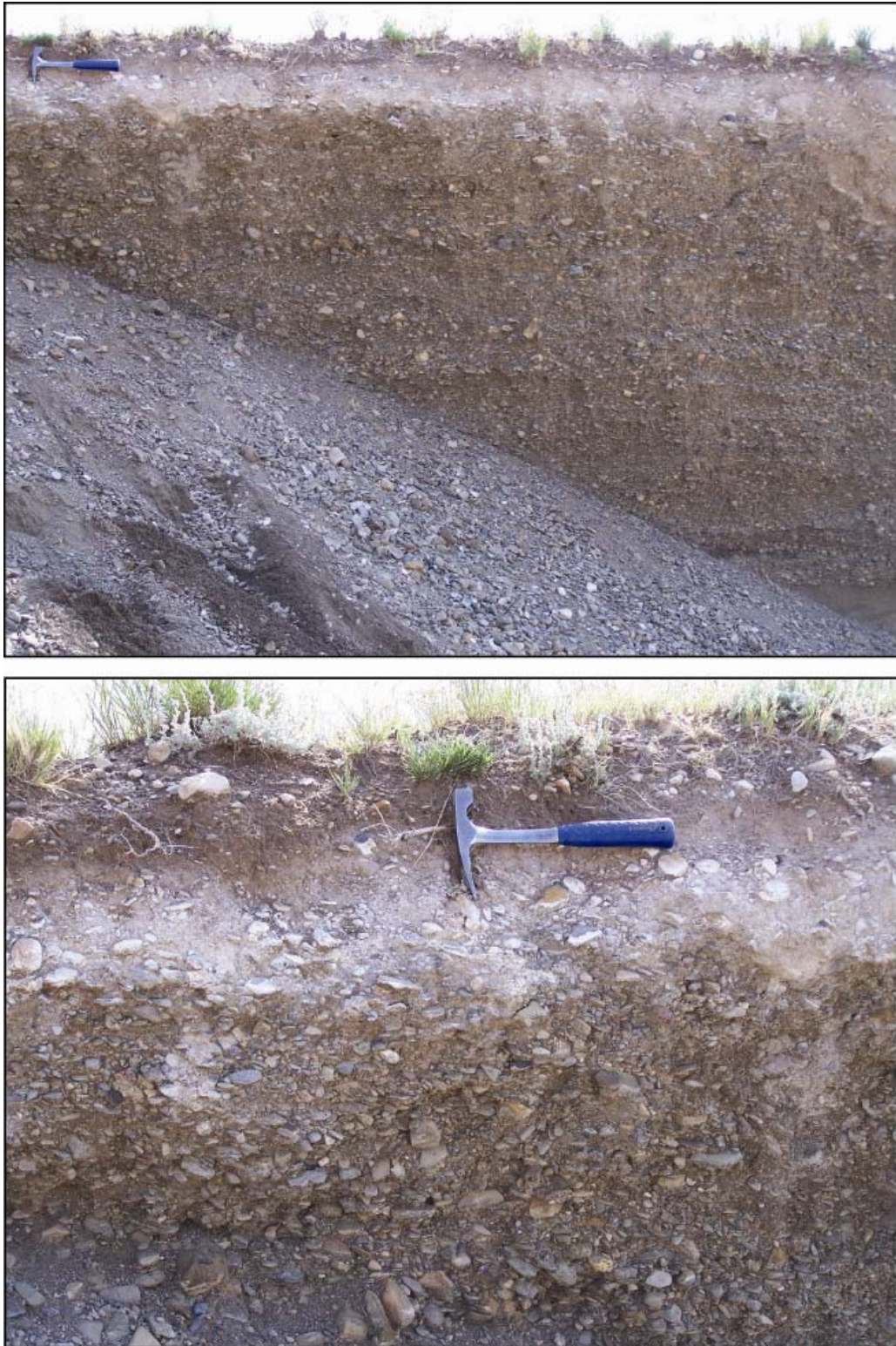


Figure 4. Exposure of unit Qa2 in an inactive gravel pit in center of the NE $\frac{1}{4}$ of section 31, T. 12 S., R. 76 W. (~UTMX: 419329, UTM Y: 4313508). Upper photograph is an overview of the exposure. Pedogenic soil shown in lower photograph includes a Bw horizon about 4 to 5 inches thick and a 5- to 6-inches-thick Bk horizon with stage II to weak stage III carbonate. The boundary between the Bw and Bk horizons is near the chisel end of the rock hammer.

that have stronger carbonate morphology. Stratigraphic relationships between alluvial unit two and the late Pleistocene tills northwest of the quadrangle (Widmann and others, 2004; 2006; 2011), along with soil development and clast weathering, suggest alluvial unit two was deposited during the Pinedale glaciation (oxygen isotope stage 2), which extended from about 13 to 35 ka.

The base of alluvial unit two is not exposed in the quadrangle, and no subsurface information was discovered that clearly described the thickness of the unit. Maximum thickness of alluvial unit three is estimated at about 30 feet.

Qa3 Alluvial unit three (late middle Pleistocene)—Deposits of alluvial unit three were recognized in Pony Park, along Buffalo Creek near highway 285, and on the northeast side of Hall Butte. No exposures of these deposits were found. The deposit in Pony Park underlies the distal end of an outwash fan associated with Pony Creek, whose headwaters in the Marmot Peak quadrangle were glaciated (note that on the topographic base map of the Marmot Peak quadrangle Spring and Pony Creeks are mislabeled). Gravel clasts preserved on the fan surface are composed chiefly of andesite and minor amounts of sedimentary rock types that apparently were derived from the Paleozoic rocks that crop out in the drainage basin of Spring Creek. Some of the volcanic clasts are decomposed. Clasts on the fan surface within the quadrangle are mostly pebble and cobble sized; however, to the west on Marmot Peak quadrangle boulders are common on the surface in the proximal part of the fan. On the basis of the soils and gravel clasts on the fan surface, the deposit probably consists of pebbly and cobbly sandy silt that may have been deposited as debris flows or hyperconcentrated flows. Thickness is uncertain, perhaps at most a few tens of feet thick.

The clasts in the deposit near highway 285 are similar in size and composition to those on the fan in Pony Park. The deposit near highway 285 is about 30 feet above Buffalo Creek and appears to be only 3 or 4 feet thick. Clasts in the deposit of unit Qa3 at the northeast end of Hall Butte are more varied in composition; they include quartzite, chert, and quartz, in addition to andesite and sandstone. These clasts are mostly subangular to subround pebbles, but some are cobbles up to about 8 inches in diameter. The sediments in unit Qa3 are inferred to have been deposited during the late middle Pleistocene Bull Lake glaciation, primarily on the basis of their position in the landscape.

Qay Younger alluvium (late and late middle Pleistocene)—Includes deposits of glacial outwash that probably were deposited in either the Pinedale or Bull Lake glacial periods, but available data are inadequate to discern which glacial period. Younger alluvium is mapped in four areas. A small deposit of younger alluvium is on the south side of Salt Creek between the Salt Works ranch and the town site of Haver; a second and larger deposit is on a low drainage divide between Spring Creek and Salt Creek west of Highway 285; a third deposit is in Chubb Park near the southwest corner of the quadrangle; and the fourth deposit is near the northeast corner of the quadrangle downstream of the Antero Reservoir dam.

Refer to alluvial units two and three for descriptions of younger alluvium. The deposit of younger alluvium near the southwest corner of the quadrangle differs from other deposits included within this map unit in that it consists chiefly of angular to subangular clasts eroded from Paleozoic sedimentary formations resting in a matrix of silt and sand. Beds within this deposit range from clast-supported to matrix-supported. Rather than being purely fluvial, the deposit near the quadrangle's southwest corner may include debris-flow sediment from drainages that are tributary to Trout Creek, in contrast to the fluvial sediment deposited by perennial streams that characterizes other deposits of younger alluvium. Evaporite karst and locally thick

accumulations of precipitate rich in gypsum obscure contacts and pedogenic soils associated with the deposit of younger alluvium near the northeast corner of the quadrangle. Thin veneers of sheetwash, Holocene alluvium, and colluvium may exist with the karst depressions formed in younger alluvium near the quadrangle's northeast corner. Deposits of younger alluvium range from about 5 to 25 feet above adjacent streams. Thickness is poorly constrained; it may be a maximum of about 20 feet.

Qa4 Alluvial unit four (middle Pleistocene) — Alluvial unit four was deposited as glacial outwash and is similar in character to alluvial unit two, with the following exceptions: (1) remnants of alluvial unit four are preserved higher in the landscape than alluvial unit two; (2) many of the Laramide intrusive and Precambrian clasts within the alluvial unit four are moderately to strongly weathered; and (3) the pedogenic soils formed on alluvial unit four typically include well developed carbonate-rich horizons. Deposits of alluvial unit four occur only near the northeast corner of the quadrangle, where they are about 60 to 80 feet above the South Fork of the South Platte River.

To the north in the Garo quadrangle, alluvial unit four was subdivided into two subunits, a younger unit (Qa4y) and an older unit (Qa4o), chiefly on the basis of their relative positions in the landscape (Kirkham and others, 2007). The deposits of alluvial unit four within the Antero Reservoir quadrangle are contiguous with and correlative to the younger alluvial unit four in the Garo quadrangle. Pedogenic soils formed on deposits of alluvial unit four include argillic Bt horizons that are several inches thick and may have prismatic structure. Locally, they have a K horizon with moderate stage III to weak stage IV morphology. Outcrop patterns suggest the thickness of alluvial unit four within the quadrangle typically is 10 to 20 feet, although thicknesses in excess of 100 feet were reported in the adjacent Garo quadrangle (Kirkham and others, 2007).

Qao Older alluvium (middle Pleistocene) — Deposits of older alluvium cap low hills on both sides of highway 285 about 1 to 2 miles north of Antero Junction and are also found on a ridge line near the northwest corner of the quadrangle adjacent to Pony Creek. The unit includes gravel and sand that probably were deposited as outwash during either the Bull Lake or pre-Bull Lake glacial periods, but available data are inadequate to discern which glacial period. No exposures of older alluvium were observed. The float present in areas mapped as older alluvium consists of subround to subangular pebbles and cobbles. Clasts within the float over deposits of older alluvium along highway 285 north of Antero Junction consists of various sedimentary rock types typical of the Paleozoic formations, as well as quartzite and sparse hornblende andesite. Clasts brought to the surface by animal burrows commonly are completely coated with pedogenic carbonate. The modern topographic configuration of the large remnant of older alluvium on the east side of the highway suggests deposition by the unnamed stream that lies east of the deposit. The deposit ranges from about 20 to 40 feet above the unnamed stream.

Float that overlies the deposits of older alluvium near the northwest corner of the quadrangle consists mostly of hornblende andesite and minor amounts of sedimentary rock types typical of the Paleozoic formations. The two deposits may be remnants of a single original unit, or they may be slightly different in age. Pony Creek has eroded about 60 to 80 feet below the older alluvium. Deposits of unit Qao probably are at most about 10 to 15 feet thick.

Mass-Wasting Deposits

Qc Colluvium (Holocene and late Pleistocene) — Colluvium consists of poorly sorted, sandy or silty, fine to coarse gravel, gravelly sand, and gravelly silt that accumulated on or at the foot of hill slopes. Colluvium can be rich in boulders below cliffs and rocky outcrops. As used here, colluvium generally follows the definition of Hilgard (1892) in that it (1) is derived locally and transported only short distances, (2) is not distributed by channelized water flow, (3) contains clasts of varying size, including boulders, (4) has little or no sedimentary structures or stratification, features which are typically caused by channelized flow of water, and (5) may include minor amounts of sheetwash and debris-flow deposits. Unit Qc also may locally include landslide deposits or talus that either are too small to differentiate at the map scale or which are difficult to clearly discern on aerial photographs. Clasts in colluvium typically are angular to subangular, except in areas where the bedrock or surficial deposits in source areas for the colluvium contain well-rounded clasts. Maximum thickness of colluvium is estimated at about 25 feet.

Qls Landslide deposits (Quaternary) — Landslide deposits consist of heterogeneous, mostly unsorted and unstratified debris and are commonly characterized by hummocky topography. Most of the landslides formed in areas where the Minturn Formation, primarily the evaporite facies, underlies volcanic rocks, such as at Hall Butte, McQuaid Butte, and Mount Hall. These landslides have failure planes in the Minturn strata but also involve overlying volcanic formations, therefore the landslide deposits typically contain large boulders of volcanic rocks. The small landslide near the southeast corner of the quadrangle formed in the Wall Mountain Tuff. A landslide deposit in Chubb Park near the southwest corner of the quadrangle consists of a block of Dyer Dolomite that rests on the Belden Shale. The block of dolomite is interpreted as a remnant of a rock slide or rock that slid off of Kaufman Ridge. Most landslides appear to be only 10 to 20 feet thick, although landslide deposits on the southeast end of McQuaid Butte may attain a thickness of about 40 feet.

Alluvial and Mass-Wasting Deposits

Qf Fan deposits (Holocene and late Pleistocene) — Fan deposits include sediment within geomorphically distinct fans that form at the mouths of tributary valleys. In some areas the deposits from adjacent valleys merge to form fan complexes. Fan deposits consist of poorly sorted, clast-supported sandy gravel and gravelly sand that was deposited as alluvium during storm events and also debris-flow deposits, which are composed of matrix-supported, poorly sorted, silty or sandy gravel. Fan deposits, especially those containing debris-flow deposits, may be rich in boulders. Clasts within fan deposits are mainly subangular to angular. Fan deposits commonly are 5 to 15 feet thick, but locally may be as much as 25 feet thick.

Qac Alluvium and colluvium (Holocene and late Pleistocene) — Unit Qac consists of alluvial sediments in channels, flood plains, and low terraces in tributary drainages and colluvium and sheetwash along valley margins and on hill slopes. The alluvial component of the unit can be very poorly sorted to well sorted, with textures that range from sandy pebble, cobble, and boulder gravel to stratified fine sand and silt. Clasts in the alluvial component are subangular to subround. The colluvial part of unit Qac typically consists of very poorly sorted, unstratified or poorly stratified, gravelly to silty sand, sandy to silty gravel, and gravelly sandy silt. Clasts in the colluvial part are chiefly angular to subangular. Locally, the unit may include

debris-flow deposits, and also small landslides or soil slips. Thickness of unit Qac is estimated to range from about 3 to 20 feet.

BEDROCK UNITS

Tertiary Sedimentary and Igneous Rocks

Tw Wagontongue Formation (Miocene) — Poorly lithified sedimentary rocks of the Wagontongue Formation crop out along the eastern margin of the quadrangle in the axial part of the Antero syncline. The Wagontongue underlies low hills that rise up 80 to 100 feet above the topographically low strike valley of the Antero Formation (Fig. 5).

The Wagontongue Formation is very poorly exposed in the quadrangle. The only exposure found was in a shallow trench on a ridge in the SW $\frac{1}{4}$ of section 19, T. 13 S., R. 76 W., where only a few feet of weakly cemented, tuffaceous, sandy cobble and pebble gravel were exposed. These sediments are clast-supported, and the clasts are subround to subangular and composed mostly of andesitic volcanic material, much of which is decomposed. Other clasts are mostly chert, quartzite, quartz, granitic rock fragments, ash-flow tuff, and potassium feldspar. In many areas, gravel float or lag laying on the ground surface consists of cobbles, pebbles, and sparse boulders up to about two feet in length. In other areas underlain by the Wagontongue Formation sand-size material dominates the soils and gravel float or lag is sparse, suggesting the underlying sediments were sandy. The Wagontongue Formation unconformably overlies the Antero Formation. On the basis of cross section A-A' the maximum thickness of the Wagontongue Formation within the quadrangle is estimated at about 1,400 feet, which is similar to the thickness of 1,300 feet that was reported by De Voto (1971).



Figure 5. Hills underlain by the Wagontongue Formation (Tw) rise up sharply from the strike valley underlain by the Antero Formation. Three Antero limestone beds (Tal) were identified in this area. One limestone bed holds up the ridge from which the photograph was taken (location ~UTMX: 423704, UTM Y: 4307019), and two more form the low ridges within the strike valley. A fourth low ridge is mantled with gravel float, which suggests a conglomeratic facies of the Antero Formation (unit Tac) may underlie that ridge.

Ta Antero Formation (Oligocene) – The Antero Formation crops out in the eastern part of the quadrangle, in a strike valley along the northwestern and eastern margins of the Antero syncline. The Antero Formation locally includes three informal facies that are mapped separately: a limestone facies, a conglomeratic facies, and an ash-flow tuff facies. The ash-flow tuff facies is present near the base of the formation along the northwest and west sides of the Antero syncline. The limestone facies consists of a single limestone interval in some areas and as many as four separate limestone intervals in other areas. A fairly continuous belt of gravelly float caps low hills within the strike valley underlain by the Antero Formation. The conglomeratic facies probably underlies these hills with gravel float.

The weakly indurated main body of the Antero Formation underlies topographically subdued areas along the eastern side of the Antero syncline and in the valley of the South Fork of the South Platte downstream of Antero Reservoir. It is poorly exposed in the quadrangle. The unit was primarily recognized on the basis of float that consists of sparse, small chips of tuffaceous mudstone and tuff. In the exposures examined during the study, the tuffaceous facies includes weakly lithified, light-gray to tan, tuffaceous mudstone that locally was iron stained, pumice-rich mudstone, and calcareous, pumice-rich, lapilli tuff with very light-gray to white rounded or slightly flattened lapilli. The lapilli are composed of about 8 to 10 % plagioclase, 2 % sanidine, 2 % biotite, 0.5 % hornblende, and accessory sphene, magnetite, and apatite. In the calcareous tuff, carbonate comprised over half of the rock, occurring both as an interlocking mosaic matrix and as a locally extensive replacement of the pumice clasts.

On the basis of paleontological evidence, previous workers assigned an early Oligocene age to the Antero Formation (for example, Brown, 1940; Stark and others, 1949; Lozano, 1965; De Voto, 1971). Recent $^{40}\text{Ar}/^{39}\text{Ar}$ dating of tuff beds and tuffaceous sediments in the Antero Formation elsewhere in the region yielded an average of 33.98 ± 0.10 Ma (McIntosh and Chapin, 2004; recalibrated to Renne and others, 1998) (see Appendix B). Sanidine from an ash-flow tuff within the Antero Formation in the quadrangle (sample A217) yielded an $^{40}\text{Ar}/^{39}\text{Ar}$ age of 34.03 ± 0.09 Ma (Table 1 and Appendix B). These absolute ages indicate the Antero Formation was deposited in early Oligocene and/or late Eocene time (Fig. 3).

The Antero Formation unconformably overlies several older formations. Maximum thickness within the quadrangle is estimated at about 1,300 feet. To the east, near the axis of the Antero syncline, De Voto (1971) reported an approximated thickness of 2,000 feet.

Table 1. $^{40}\text{Ar}/^{39}\text{Ar}$ ages of igneous rocks in the Antero Reservoir quadrangle. See Appendix B for geochronology report on samples A129, A217, and A320. Age of sample A983 provided by M.J. Kunk (written communication, 2011; recalibrated using a monitor age of 28.02 Ma for the Fish Canyon Tuff, as recommended by Renne and others, 1998). Sample locations are described in Appendix A and shown on the geologic map (Plate 1).

Unit	Age	Material dated
Tat	34.03 ± 0.09 Ma (sample A217)	sanidine
andesite boulder or flow in Ttc	37.07 ± 0.20 Ma (sample A320)	biotite
Tva	37.84 ± 0.19 Ma (sample A129)	hornblende
Ti	60.95 ± 0.15 Ma (sample A983)	sanidine

Tal Limestone facies — The limestone facies of the Antero Formation consists of as many as four separate limestone intervals within the middle and upper parts of the tuffaceous facies of the Antero Formation. The limestone facies appears to be absent in parts of the strike belt of the Antero Formation. Some limestone beds locally form prominent outcrops (Fig. 6), but in most areas the limestone interval is poorly exposed. In areas of poor exposure the unit was mapped on the basis of limestone float that mantled subtle ridges within the topographically low strike valley of the Antero Formation. Because of this, rock types other than limestone may exist within areas mapped as the limestone facies. Antero limestone beds are locally replaced with silica that can be very attractive and may be of lapidary quality.

Antero limestones typically are light-gray to tan, impure, microcrystalline limestone that is commonly recrystallized to a purer, coarse-grained calcite. The impurity is a disseminated, white, opaque mineral that possibly is anatase or leucoxene. Crystals of feldspar, probably reworked from the volcanic tephra that fell into the lake, are relatively common. Antero limestones commonly are rich in ooids, some of which are quite large and possibly oncolites. Some ooids have nuclei of feldspar; others have peloids of microcrystalline calcite with white opaque minerals and siliciclastic grains. Ostracod carapaces are also common constituents. In some samples, articulated carapaces occur in a matrix of partially recrystallized micrite. In others, disarticulated carapaces with weak preferred orientations occur with ooids. Void spaces in oolitic samples are filled with sparry calcite cement. The distinctive algal features reported by Johnson (1937a, b) in Antero limestone beds elsewhere in South Park were not observed in the quadrangle. Individual limestone intervals attain a maximum thickness estimated at 120 feet.



Figure 6. Limestone beds in the Antero Formation usually underlie small ridges and locally form fair outcrops. At this location about 1,800 feet southeast of the junction of county roads 55 and 101 the limestone bed is partially replaced with silica (location ~UTMX: 423567, UTM Y: 4307588).

Tac Conglomeratic facies — A somewhat laterally persistent low ridge covered with locally abundant pebble- and cobble-sized float exists along the northwest side of the Antero syncline. This area is interpreted to be underlain by a conglomeratic facies within the Antero Formation. In places the clasts in the float are composed nearly entirely of chalcedony; elsewhere they are chiefly andesite, ash-flow tuff, and granitic fragments. A single exposure of the strata that underlies the area with gravel float was discovered in the quadrangle along the northwest side of Highway 24 in section 34. There the few feet of exposed strata consist of weakly lithified pebbly sandstone. Maximum thickness of the conglomeratic facies is estimated at about 100 feet.

Tat Ash-flow tuff facies — Intermittent outcrops of crystal-rich ash-flow tuff exist in the lower part of the Antero Formation from about one-half mile south of Highway 24 northeast to the east edge of the quadrangle. The outcrop pattern, as well as the petrology of the rock, suggests the remnants are from a single ignimbrite sheet, and that the tuff either partially filled paleovalleys and did not lap over drainage divides or it originally blanketed the ground surface and subsequently was partially removed by erosion after eruption. The light-brown to medium-yellow-brown tuff has a salt-and-pepper appearance due to the presence of light- and dark-colored phenocrysts. Plagioclase is the dominant phenocryst, composing about 28 to 34 % of the rock. Other phenocrysts include sanidine (6 to 9 %), biotite (4 to 7 %), hornblende (2 to 5 %), and magnetite (trace to 2 %), with accessory sphene, apatite, allanite, and zircon. Accidental crystals and lithic clasts comprise 3 to 10 % of the rock. Little or no evidence of collapsed pumice clasts was noted. Most vitroclastic textures have been destroyed by devitrification. Micro-botryoidal structure is present in samples.

Three samples of ash-flow tuff in the Antero Formation were chemically analyzed (see Appendix A, samples A217, A236, and A288). The tuff contains 66 to 69 % silica and 5 to 6 % total alkali (water and volatile free and summed to 100 %). All three samples plot in the dacite field of a total alkali-silica diagram (Fig. 7).

Sanidine from sample A217 yielded an $^{40}\text{Ar}/^{39}\text{Ar}$ age of 34.03 ± 0.09 Ma using single-crystal laser fusion methods (Table 1 and Appendix B). This age is within the error of the 33.98 ± 0.10 Ma age of the Antero Tuff reported by McIntosh and Chapin (2004) (recalibrated to Renne and others, 1998) (see Appendix B).

A complete exposure of the entire ash-flow tuff facies was not found. The maximum thickness of the ash-flow tuff facies is estimated at about 50 feet.

Tlm Unnamed limestone (Oligocene or Eocene) — A fairly continuous belt of limestone extends southeastward from the south abutment of the dam at Antero Reservoir and then wraps around the southern side of the hills between the reservoir and U.S. Highway 24. Near the reservoir the limestone unconformably overlies the Minturn Formation. To the south, and also on the south side of the hills between the reservoir and the highway, the limestone rests either on the Wall Mountain Tuff, Minturn Formation, or Tallahassee Creek Formation. The unit varies in composition, but typically consists of light-gray to tan, laminated, sparry limestone or vuggy calcareous tufa, which locally is moderately to strongly silicified (Fig. 8).

Light-colored bands of laminated limestone are fairly pure, coarsely crystalline calcite. A finer-grained ferroan calcite composes most dark-colored bands. Fractures are filled with coarsely crystalline relatively pure calcite. Fibrous chalcedony locally replaces the crystalline calcite. In some places voids within the limestone are filled with chalcedony that has a botryoidal

texture. Locally, a whitish opaque mineral (anatase or leucoxene?) is finely disseminated in the calcite. The limestone locally has been subjected to multiple generations of silification. One sample shows three generations of fibrous chalcedony, one generation of equant quartz crystals, and a final generation of coarsely crystalline, equant, sparry calcite cement.

The age of the unit is uncertain. It could be within the base of the Eocene Tallahassee Creek Conglomerate, as indicated by De Voto (1971) and Scott (2008), but it could also be interpreted as a spring deposit that formed along the margin of Oligocene-age “Lake Antero” either early or late during the life of the lake. The estimated maximum thickness of the unit is about 40 feet; however, it is commonly much thinner.

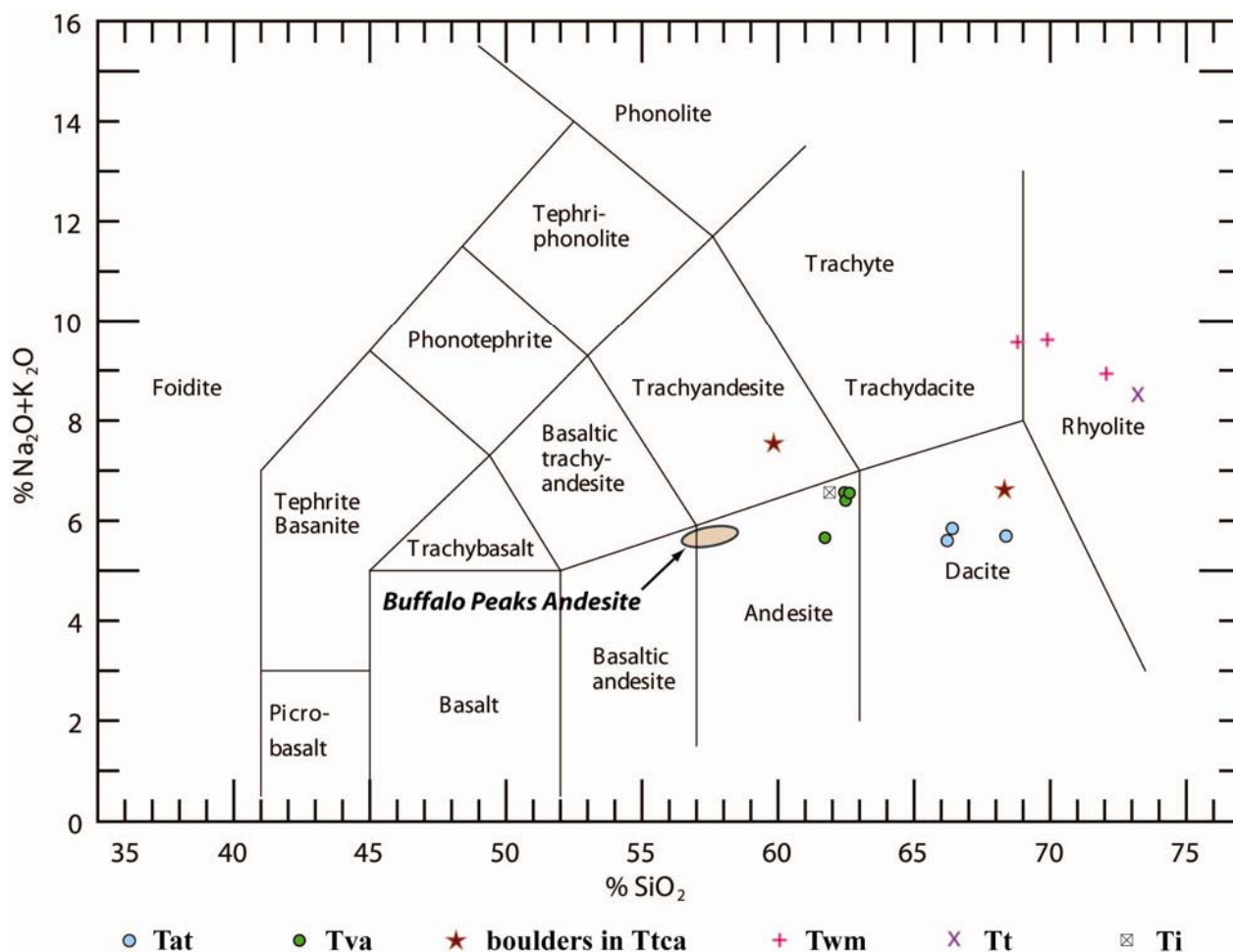


Figure 7. Total alkali-silica diagram of volcanic and selected intrusive rock samples from the Antero Reservoir quadrangle and the Buffalo Peaks Andesite. The symbols are keyed to the unit symbols on the map. Samples from the Buffalo Peaks Andesite that were collected on Buffalo Peaks contain significantly less total alkali and slightly less silica than the samples from unit Tva collected in the quadrangle. The analysis of the porphyry intrusion (Ti) is included to allow for comparisons with the chemistry of the volcanic rocks. Classification scheme is that of Le Bas and others (1986). Values are in weight percent and are water and volatile free and summed to 100%. See Appendix A for the geochemical analyses of samples from the quadrangle. These sample locations are described in Appendix A and shown on the geologic map (Plate 1). Analytical data for the samples of Buffalo Peaks Andesite are from Campbell (1994), Widmann and others (2011), and Houck and others (in preparation).



Figure 8. The unnamed Tertiary limestone unit (Tlm) commonly is composed of laminated sparry limestone (upper photograph) or vuggy calcareous tufa (lower photograph), which locally is moderately to strongly silicified. Chalcedony-filled vugs typically have a botryoidal texture.

Ttc Tallahassee Creek Conglomerate (Eocene) — The Tallahassee Creek Conglomerate crops out along the western flank of the Antero syncline and on the hill slopes adjacent to Mount Hall, Hall Butte, and McQuaid Butte. The unit is widespread in the southeast part of the quadrangle where it unconformably overlies the Wall Mountain Tuff or Pennsylvanian age sediments in the Minturn Formation. Elsewhere, it occurs only as scattered remnants. The Tallahassee Creek Conglomerate was called the “lower volcanic conglomerate” by De Voto (1971).

The unit is generally poorly exposed. Its extent was mapped primarily on the basis of gravel float that commonly included boulders of granitic rocks or ash-flow tuff up to about 20 feet in length (Fig. 9) and also silicified, locally opalized, petrified wood.

Although the Tallahassee Creek Conglomerate is typically poorly lithified and poorly exposed, locally it is sufficiently well cemented to form low ridges. In these exposures the non-calcareous formation ranges from clast-supported pebble conglomerate with graded bedding to matrix-supported, conglomeratic, sandy mudstone. Where exposed, the conglomerate clasts are commonly subround to subangular and composed mostly of andesitic volcanic rocks, ash-flow tuff (probably Wall Mountain Tuff), quartz, potassium feldspar, and granitic rocks. In contrast, road cuts and other human-made exposures near the southwest corner of section 9, T. 13 S., R. 76 W. revealed only fine-grained strata that are weakly cemented non-calcareous siltstone, silty very fine sandstone, and matrix-supported conglomeratic siltstone. The formation may contain considerable fine-grained strata, even in areas that are mantled by abundant gravel float. No exposures of strata rich in boulders were observed in the quadrangle, but the size of the boulders suggests transport by debris flows or by water moving at very high velocity.

In the SW $\frac{1}{4}$ of section 4 and the NW $\frac{1}{4}$ of section 9, T. 13 S., R. 76 W. there are small lens-shaped areas where the float overlying the Tallahassee Creek Conglomerate consists almost entirely of intermediate-composition volcanic clasts, some of which are very large (>20 feet in length). These areas are depicted on Plate 1 by a dark gray color within or adjacent to the light-purple color used for polygons of Tallahassee Creek Conglomerate. In hand specimen and in thin section these clasts appear to be andesitic. Phenocrysts compose up to about 50 % of the rock. Nearly all of the phenocrysts are plagioclase, some of which are strongly resorbed. Augite, biotite, and perhaps magnetite also occur as phenocrysts, but in relatively small amounts. The groundmass is fine grained and glassy. Most of the glass is devitrified.

To assess whether these lens-shaped areas of float with very large boulders of andesite were from volcanic flows intercalated with the sediments within the Tallahassee Creek Conglomerate or from beds of very coarse-grained boulder conglomerate that were composed almost entirely of intermediate-composition volcanic clasts, two of these clasts (samples A320 and A324) were chemically analyzed, and one sample (A320) was dated using $^{40}\text{Ar}/^{39}\text{Ar}$ methods. Sample A324 contained 59.7 % silica and 7.5 % total alkali (water and volatile free and summed to 100 %) and plotted in the trachyandesite field of the TAS diagram (Fig. 8). In contrast, sample A320 had 68.3 % silica dioxide, 6.6 % total alkali, and plotted in the dacite field. Several other major element concentrations in these two samples also varied significantly; hence the two samples apparently are from different volcanic flows.

Biotite from sample A320 yielded an $^{40}\text{Ar}/^{39}\text{Ar}$ age of 37.07 ± 0.20 Ma using the furnace incremental heating age spectrum method (Table 1 and Appendix B). If sample A320 was significantly younger than the Wall Mountain Tuff, then sample A320 could be from a volcanic

flow within the Tallahassee Creek Conglomerate. But if sample A320 was significantly older than the Wall Mountain Tuff, then it probably would be from a boulder conglomerate within the Tallahassee Creek Conglomerate. Unfortunately, the age of biotite from sample A320 is within the error of the generally accepted age of 36.93 ± 0.09 Ma on sanidine from the Wall Mountain Tuff (recalibrated from McIntosh and Chapin, 2004). The new age determination does not provide conclusive evidence as to whether the samples came from volcanic flows or boulder conglomerates in the Tallahassee Creek, but the chemistry of the two analyzed samples suggests the lens-shaped areas are float from boulder conglomerates that are rich in andesitic clasts.

Some of the ridges underlain by the Tallahassee Creek Conglomerate south of the south edge of the quadrangle were mistakenly mapped as Wall Mountain Tuff by Wallace and Keller (2003). Near the center of section 33, T. 13 S., R. 76 W. the Tallahassee Creek Conglomerate includes a lens of microcrystalline limestone that is rich with ostracods, but the lens appears to end before reaching the south end of the quadrangle. De Voto (1971) and Scott (2008) mapped a localized limestone member within the Tallahassee Creek Formation between Antero Reservoir and Highway 24; however, we suspect these rocks may be younger than the Tallahassee Creek Conglomerate and therefore include them in a separate formation (unit Tlm). Areas mapped by De Voto as limestone within the Tallahassee Creek Conglomerate in section 21, T. 13 S., R. 76 W. are silicified zones that could originally have been limestone or possibly tuff. The silicified zones at the base of the Tallahassee Creek in section 33 of the same township also may have been limestone or tuff.

Maximum thickness of the Tallahassee Creek Conglomerate is uncertain. In many areas it appears to mantle the ground surface and perhaps be only at most a few tens of feet thick. Elsewhere map relations and cross sections suggest a thickness of as much as about 800 feet, which agrees with the estimate of De Voto (1971).



Figure 9. The Tallahassee Creek Conglomerate includes boulders as much as 20 feet long (upper photograph; location ~UTMX: 421584, UTM Y: 4311887; black pack is 2 feet long). In most areas underlain by the formation, such as the hill in the middle distance of the lower photograph, the ground surface is littered with cobbles and boulders (location ~UTMX: 418815; UTM Y: 4312455). As seen in the foreground of the lower photograph, colluvium or lag from the formation also can mantle the ground surface in areas adjacent to the formation.

Twm Wall Mountain Tuff (Eocene) — Large remnants of the Wall Mountain Tuff are preserved along the west flank of the Antero syncline and on Mount Hall. Small remnants also exist on the east ends of Hall Butte and McQuaid Butte. The formation is a devitrified, densely welded, pink to light-purple, vitric-crystal-lithic, ash-flow tuff that usually forms prominent outcrops and caps hills. It has remnant glass shard textures, although the glass is completely devitrified. A glassy vitrophyre is locally present at the base of the unit. Collapsed pumice clasts comprise 5 to 20 % of the tuff. Phenocrysts within the rock are large and abundant. Sanidine is the most common phenocryst (14 to 15 % of the rock by volume), and plagioclase also is abundant (12 to 13 %), yielding a sanidine:plagioclase ratio that falls within the typical range for the Wall Mountain Tuff (McIntosh and Chapin, 2004). Biotite phenocrysts compose about 1 to 3 % of the rock. Some samples contained minor amounts of augite and hornblende,

which is typical of the Wall Mountain Tuff; however, augite and hornblende were absent in other samples from this formation.

Three whole-rock samples of the Wall Mountain Tuff from the quadrangle were chemically analyzed (samples A142, A166, A348; see Appendix A). The silica content ranged from about 69 to 72 %, and total alkali content varied from 8.8 to 9.7 % (water and volatile free and summed to 100 %). Two of the three samples plot in the rhyolite field of the total alkali-silica diagram, and the third plots in the trachydacite field adjacent to the rhyolite field (Fig. 7). The silica and alkali values of the samples of Wall Mountain Tuff from the Antero Reservoir quadrangle are very similar to samples of Wall Mountain Tuff from the Garo quadrangle (Kirkham and others, 2007).

McIntosh and Chapin (2004) reported an average $^{40}\text{Ar}/^{39}\text{Ar}$ age of 36.69 ± 0.09 Ma for the Wall Mountain Tuff on the basis of single-crystal dating of sanidine from five samples that were collected elsewhere in the region. Using a monitor age of 28.02 Ma for the Fish Canyon Tuff (Renne and others, 1998), the recalibrated age of the Wall Mountain Tuff reported by McIntosh and Chapin (2004) would be 36.93 ± 0.09 Ma, which is similar to the 36.93 ± 0.11 Ma age of sanidine from a sample of Wall Mountain Tuff in the Lone Hills north of the quadrangle (Kirkham and others, 2007). Maximum thickness of the Wall Mountain Tuff is estimated at about 200 feet.

Tt Unnamed tuff (Eocene?) — A single small outcrop of medium-gray-brown, welded, ash-flow tuff near the southeast corner of the quadrangle is included in unit Tt. The tuff outcrop is adjacent to outcrops of the Wall Mountain Tuff, but it may be a different ignimbrite. It differs from the Wall Mountain Tuff in that it has significantly fewer phenocrysts, and the phenocrysts are much smaller. The sanidine:plagioclase ratio is very high, much higher than the typical ratio in the Wall Mountain. The unnamed tuff also contains abundant biotite phenocrysts, has more accidental crystals including quartz and microcline, has a well-developed vitroclastic texture with microspherulites in pumice clasts, and lacks augite and hornblende.

A single sample of unit Tt was chemically analyzed (sample A391). It contained slightly more silica (73 %) and slightly less total alkali (8.4 %) than samples of Wall Mountain Tuff collected within the quadrangle (Fig. 7) and in the adjacent Garo quadrangle (Kirkham and others, 2007). Chiefly on the basis of petrography, the tuff does not correlate well with any other known ignimbrite (J. R. Shannon, 2007, written communication). Field relationships suggest the unnamed tuff underlies and is older than the Wall Mountain Tuff, but an unrecognized fault potentially could separate the two units, in which case the age relationships might be reversed. Also, there could be compositional zoning within the Wall Mountain Tuff that we have not recognized, in which case tuff unit Tt might be part of the Wall Mountain Tuff. Exposed thickness is about 10 feet.

Tva Andesitic volcanic rocks (Eocene) — A thick sequence of light- to medium-gray, porphyritic, andesitic lava flows, flow breccias, and minor lahars caps McQuaid Butte and Hall Butte. The flow sequence is relatively intact on McQuaid Butte, where individual flows locally form good outcrops that can be traced as much as several hundred feet. On Hall Butte the flows are poorly exposed and difficult to trace laterally.

Phenocrysts usually comprise almost 50 % of the rock. The most common phenocrysts are large, partially resorbed plagioclase, mostly of andesine or calcic andesine composition, and large, partially resorbed, reddish hornblende, commonly with oxide reaction rims or magnetite

rims. The smaller phenocrysts include pyroxene (both hypersthene and augite), magnetite, biotite, and plagioclase. The groundmass typically has an intergranular texture with laths of plagioclase, blocky pyroxene (probably augite), blocky magnetite, and minor ilmenite. In some samples the plagioclase phenocrysts are flow aligned.

Chemically these rocks contain around 62 % silica and 5.6 to 6.6 % total alkali (water and volatile free basis and summed to 100 %; samples A129, A133, A137, A146; Appendix A). All four samples of unit Tva plot in a tight cluster in the high-silica and high-alkali part of the andesite field in the total alkali-silica diagram (Fig. 7).

Field relationships do not clearly define the stratigraphic relationships between the andesitic rocks of unit Tva and the Wall Mountain Tuff and Tallahassee Creek Conglomerate. Prior publications did not consistently characterize the stratigraphic relationships of these units. To evaluate the age and stratigraphic relationships between unit Tva and the Wall Mountain Tuff and Tallahassee Creek Conglomerate, a sample from unit Tva was dated using $^{40}\text{Ar}/^{39}\text{Ar}$ methods (Appendix B). Sample A129, which was collected from an andesitic flow on McQuaid Butte, yielded an age of 37.84 ± 0.19 Ma using the furnace incremental heating age spectrum method (Table 1 and Appendix B). This indicates the eruption of this andesitic flow predates both the Tallahassee Creek Conglomerate and the Wall Mountain Tuff.

Map patterns on the north side of McQuaid Butte suggest the maximum thickness of unit Tva exceeds 500 feet at that location. Elsewhere it appears to range from about 200 to 300 feet thick.

Ti Porphyritic intrusion (Paleocene) — A fine-grained, slightly porphyritic, tan-colored, narrow stock and associated dikes crop out along the Trout Creek fault in the southwest part of the quadrangle. The largest phenocrysts appear to be potassium feldspar, and the smaller phenocrysts probably are plagioclase. The groundmass is holocrystalline and composed mostly of blocky feldspars with very little quartz and minor clots of oxides that may have replaced augite. Chemically, the rock is about 62 % silica and 6.6 % total alkali (sample A983; water and volatile free and summed to 100%). On the basis of CIPW norms, the rock is classified as a monzonite. Sample A983 plots in the upper right-hand corner of the andesite field in a TAS diagram (Fig. 7), near the boundary with the trachyandesite, trachydacite, and dacite fields. An unpublished $^{40}\text{Ar}/^{39}\text{Ar}$ age of 60.95 ± 0.15 Ma was obtained by laser-fusion dating of 17 sanidine crystals from sample A983 by M. J. Kunk (written communication, 2011; recalibrated using a monitor age of 28.02 Ma for the Fish Canyon Tuff, as recommended by Renne and others, 1998), indicating the intrusion is Paleocene in age and was emplaced during the Laramide Orogeny.

Paleozoic Sedimentary Rocks

PPm Maroon Formation (Lower Permian to Upper and Middle Pennsylvanian) — This formation crops out in the Pony Park syncline in the west-central part of the quadrangle and on the north side of Antero Reservoir. Sandstone, siltstone, and mudstone are the most common rock types. Many layers are red-brown in color, but gray, gray-green, pink, and tan beds are also common. Sandstone layers are arkosic and micaceous, with silica and/or calcite cement. Plant debris occurs on some bedding planes. Fine-grained sandstone and siltstone layers are planar-laminated, ripple cross-laminated, or thinly bedded. Asymmetric ripple marks are common on bedding planes. Medium- and coarse-grained sandstone layers tend to be lens-shaped. Beds are about one to two feet thick; mud chip lags, trough cross-bedding, and soft-sediment deformation

are common. Siltstone and mudstone beds weather to red, silty soil. Sandstone beds form small ridges and flatirons.

No complete sections of the Maroon Formation occur within the Antero Reservoir quadrangle. The lowest approximately 1,000 feet of the formation are exposed in the Trout Creek syncline, and approximately 500 feet are exposed north of Antero Reservoir. In the Fairplay East quadrangle to the north, the Maroon Formation is about 5,300 to 5,600 feet thick (Kirkham and others, 2006). The Maroon Formation is thought to conformably overlie the Minturn Formation (Tweto, 1949; Tweto and Lovering, 1977).

Minturn Formation (Middle Pennsylvanian) — This formation contains a variety of rock types, including conglomerate, sandstone, siltstone, shale, limestone, dolomite, and gypsum. It probably contains halite in the subsurface and perhaps other evaporite minerals as well. There are no complete sections of the formation exposed on the quadrangle, but composite sections on adjoining quadrangles suggest a total thickness of about 5,500 to 6,000 feet for the entire formation. We divide the Minturn Formation into three major map units: an upper interval, a lower interval, and the Coffman Member, which lies between the upper and lower intervals. The Coffman Member is the only formally recognized member of the Minturn in the quadrangle. We also recognize and map an evaporite facies in the basal part of the upper interval. We also map individual limestone beds within the upper interval, including those in the evaporite facies.

Pmu Upper interval — The upper interval crops out in the Pony Park syncline in the west-central part of the quadrangle, as well as in the northwest and northeast parts of the quadrangle. Stratigraphically it comprises the upper 4,500 to 5,000 feet of the formation. The upper interval includes an evaporite facies that is described below. Common rock types in the upper interval are sandstone, siltstone, shale, calcareous shale, limestone, and gypsiferous shale. Some conglomeratic sandstone occurs in the northwestern part of the quadrangle. Sandstone layers are red-brown, pink, tan, gray, or greenish. Thick layers form ridges and small cliffs. They are micaceous and arkosic. Some contain plant debris (Fig. 10). Mud chips and small limestone pebbles are also present at some horizons. Siltstone and fine sandstone beds are commonly planar-laminated or ripple cross-laminated in six to eight-inch beds. Sedimentary structures include asymmetric ripple marks, rain drop impressions, mud cracks, invertebrate trails, and bioturbation. Medium- to coarse-grained and conglomeratic sandstone layers are commonly lens-shaped, and are up to 30 feet thick. Individual beds are up to three feet thick. Sedimentary structures include planar bedding, trough cross-bedding, and complex irregular folds caused by soft-sediment deformation.

Limestone beds are typically gray, micritic, and about three inches to one foot thick. They are especially well exposed in the parking area near the south abutment of the dam for Antero Reservoir (Fig. 11). Detrital sand, intraclasts, and algal laminations are common. The top of the upper member of the Minturn Formation is placed at the top of a thick (approximately 200 feet) layer of calcareous and gypsiferous shale that occurs at the stratigraphic position of the Jacque Mountain Limestone Member of Tweto (1949).

Pme Evaporite facies — This facies within the upper interval crops out locally across much of the quadrangle. Shale, siltstone, sandstone, gypsum, gypsiferous shale, dolomite, and limestone are the most common rock types exposed at the surface. The chemistry of the spring at the Saltworks Ranch (George and others,

1920) suggests halite and sylvite may exist within the evaporite facies in the subsurface and are dissolving. The evaporite facies commonly underlies valleys and is poorly exposed; the best exposures are on the slopes of volcanic-capped buttes (McQuaid Butte, Hall Butte, and Mount Hall). Shale and siltstone layers are gray and thinly laminated or ripple cross-laminated. Sandstone layers are generally thin, fine-grained, tan, and laminated or ripple cross-laminated. Gypsum layers are commonly around five feet thick, but are locally as much as about 50 feet thick. The gypsum is gray, black, or white. It may be thickly laminated, coarsely crystalline, or brecciated. It weathers to hard, gray, very calcareous soil with little vegetation. Microbial soils, sinkholes, and collapse structures are present. Limestone and dolomite beds within the evaporite facies range from 6 inches to three feet thick and are gray to black. Some are microcrystalline or have algal laminae and mud cracks. Others are coarsely crystalline and vuggy, like scoriaceous lava (Fig. 12). The evaporite facies is complexly deformed in the quadrangle, and its total stratigraphic thickness is unknown. It probably exceeds 1,000 feet in thickness.



Figure 10. Plant fossils are locally preserved in sandstones beds in the upper member of the Minturn Formation. (location ~UTMX: 414445; UTM Y: 4307980)



Figure 11. Limestone beds in the upper interval of the Minturn Formation are well exposed in the parking area near the south end of the Antero Reservoir dam, which forms the skyline in this photograph. View is to the north. (location ~UTMX: 422490; UTM Y: 4315160)



Figure 12. Vuggy limestone in the evaporite facies of the Minturn Formation has the appearance of scoriaceous lava. (location ~UTMX: 417610; UTM Y: 4312805)

¶mc Coffman Member – This member crops out in the central and southern parts of the quadrangle. The type section is in Kaufman Pasture in the southwest part of the quadrangle (Gould, 1935). Rock types include conglomerate, sandstone, shale, dolomite, and limestone. Most sandstone and conglomerate layers are tan, but gray, red-brown, and green-brown layers also occur. Conglomerates and conglomeratic sandstones commonly consist of gravel in a sandy matrix. The average gravel clast size is about 0.5 inches in diameter, but one to two inch pebbles are numerous, and cobbles up to four inches in diameter are common. Sand is fine, medium, or coarse grained. The Coffman Member is arkosic and micaceous, although some sandstone beds are quartz-rich or subarkosic. The gravel clasts include granite, granitic gneiss, vein quartz, and potassium feldspar. Near the base of the member, quartzite and black chert clasts are also common. Sandstones and conglomerates occur together in tabular layers three to ten feet thick. They weather to form small ridges and hogbacks with conifers growing on them. Planar beds within the layers are commonly one to three inches thick. Trough cross-bed sets are six inches to one foot thick, and planar cross-beds are two to three feet thick. Lag deposits are common at the bases of the conglomerate beds; asymmetric ripples and mud cracks occur on the tops of some of the sandstone beds.

Shale layers are dark gray to black. They are clay-rich and fissile. Some are carbonaceous, and plant debris is common. They weather to soft, noncalcareous, reddish-brown soil on gentle, grassy slopes. Limestone and dolomite layers are dark gray, black, or tan. Some have algal laminae; the others are microcrystalline. These layers are about six inches to one foot thick.

The thickness of the Coffman Member is about 700 to 800 feet, and this thickness is fairly uniform in the quadrangle. The lower contact is placed at the base of the first conglomerate bed. The member is overlain by the evaporite facies in the basal part of the upper interval in this quadrangle, and the upper contact is placed at the change from soft, brown, noncalcareous soil typical of the Coffman to hard, gray, gypsiferous and calcareous soil typical of the evaporite facies.

¶ml Lower interval – This interval crops out in the central and southern parts of the quadrangle. It is composed of sandstone and shale. Sandstone layers are medium to dark brown, greenish brown, or light gray. They are tabular and are about one to ten feet thick. The thicker layers weather to form small ridges and hogbacks with conifers on them. The sand is arkosic and micaceous with calcite cement. It is fine-grained to coarse-grained and is slightly granular in places. Sandstone beds within the layers are about three to six inches thick and are planar-laminated, ripple cross-laminated, or trough cross-bedded. Mud cracks are present on the tops of some beds. Petrified wood, plant debris, and shale rip-up clasts were found in some of the sandstone beds. Shale layers are fissile and are dark greenish gray to black. Some are carbonaceous, and some contain fish coprolites (Johnson, 1934). Shale layers weather to form gentle, grassy slopes with soft, reddish-brown, noncalcareous soil. Thickness of the lower interval is estimated at 200 feet.

¶b Belden Shale (Middle and Lower Pennsylvanian) – Consists of interbedded shale, limestone, and siltstone. The shale facies is dark gray to black, with some blue-gray calcareous shale. Shale is highly fissile, thin bedded, breaks into angular shapes, and locally calcareous. Some thin carbonaceous shale beds are locally present in Chubb Park. Non-fissile, dark-gray

siltstone and silty shale weather tan and form low semi-resistant ridges. Fissile shale beds form saddles and topographic lows between the more resistant siltstone and limestone beds. Shale beds are three to 45 feet.

Interbedded limestones are dark gray to brown and weather light gray to blue-gray. White calcite veining is common on bedding planes. The limestones reportedly contain marine fossils and stromatolites locally on the west side of Trout Creek Pass (Johnson, 1940). Abundant stromatolites with pisoliths, pellets, and ellipse-shaped concretions were found on the SW $\frac{1}{4}$ NE $\frac{1}{4}$ of section 22, T. 13 S., R. 77 W. and along Salt Creek Road near the boundary with the Marmot Peak quadrangle. Limestone beds are typically 0.5 to 3 feet thick and form small erosion-resistant ridges. A small fold in Kaufman Pasture in the SW $\frac{1}{4}$ NW $\frac{1}{4}$ of section 31, T. 13 S., R. 76 W. is easily recognized by a Belden limestone bed 0.5 to 1 feet thick.

The Newett Limestone Member of Gould (1935) was observed in the lower part of the Belden Formation on the northeast side of Kaufman Ridge. The base of the Newett Limestone Member is approximately 75 feet above the contact with the Leadville Limestone, and the member is up to 14 feet thick. This member forms a small prominent ridge between shale valleys on the west side of Kaufman Pasture.

Sandstone beds are medium-dark brown to greenish-brown and light gray, mostly fine grained, and weather light brown to rust brown. Sandstone beds are thin bedded, 0.3 to 0.8 inches thick, siliceous, and highly micaceous, with some rip-up clasts and rare mud cracks. Most beds have planar cross-laminations with faint ripple marks.

Thickness of the Belden Shale is estimated at 850 feet.

Ml Leadville Limestone (Lower Mississippian) — Consists of blue-gray to gray, massive, fine-grained dolomite that is locally dark gray to black. The formation includes local patches of “zebra rock”, which consists of irregular and alternating 0.04- to 0.08-inch-thick bands of dark-gray to black dolomite and white, coarse-grained, vuggy dolomite. On the north and east sides of Kaufman Ridge some well-rounded to angular black and/or red chert nodules (0.5 to 4 inches long) and thin calcite veins are found in lenticular siliceous beds. The Leadville Limestone on Kaufman Ridge is crystalline dolomite and micrite or dolomicrite. Some lenticular interbeds of biomicrite and silica-cemented white quartz arenite beds exist within the upper part of the formation on the east side of Kaufman Ridge near the boundary with the Castle Rock Gulch quadrangle. The quartz arenite beds are interbedded with dolomite, suggesting continuous deposition of clastic and carbonate beds at the top of the formation. The sandstone is fine to medium grained. It occurs on the crest of Kaufman Ridge in the SW $\frac{1}{4}$ SW $\frac{1}{4}$ of section 23, T. 13 S., R. 77 W. The base of the unit commonly has a mottled or brecciated appearance. The breccia typically occurs along bedding planes.

Weathered surfaces commonly are highly pitted. Soils formed on the Leadville Limestone are reddish brown. Brecciated beds show bulbous, rounded features with no bedding. The formation is resistant to erosion and forms flatiron topography on dip slopes on the north and east sides of Kaufman Ridge. Thickness of the formation is estimated at about 270 feet. The contact with the underlying Dyer Dolomite is disconformable (DeVoto, 1971).

Dc Chaffee Group (Upper Devonian) — Composed of dolomite, limestone, sandstone, dolomitic sandstone, and shale. The Chaffee Group includes the Dyer Dolomite and the Parting Formation, which are mapped separately in some areas. Total thickness of the Chaffee Group is estimated at 260 feet.

Dd Dyer Dolomite — Consists of medium- to dark-gray dolomite, massive to faint thinly bedded, micritic dolomite, micritic limestone, and minor dolomitic shale. The upper part of the formation tends to be darker than the rest of the formation. Bulbous altered chert breccias with light-gray, orange, red, dark-red-brown, yellow, tan, and brown jasperoid are locally present. Angular chert fragments up to 2 inches in diameter are in a matrix of dolomite. The lower part of the formation consists of light-gray, nodular, crystalline, vuggy limestone. Thin lenses of shale and/or chert occur locally. Weathered surfaces are soft, smooth, and yellowish to brownish gray.

The mineralized jasperoid is typically oxidized red and orange in a breccia matrix. Where brecciated, the Dyer Dolomite forms resistant outcrops over the adjacent strata, and may be mapped on the basis of float. Average thickness of the formation is estimated at 180 feet.

Dp Parting Formation — The Parting Formation is an opaque, white to light-gray, orange-brown, or tan, fine- to medium-grained, locally coarse-grained, well-sorted, quartz arenite with interbeds of tan dolomitic sandstone. Quartz pebbles may be present, especially near the base of the formation. It weathers orangish-yellow and light gray. The siliceous sandstone contains less feldspar and mica than the dolomitic sandstone. Micaceous green shales with discontinuous lenses of quartzite, and gray, sandy micritic dolomite also are common. Beds range in thickness from 0.2 to 1.0 feet thick.

The Parting Formation is less resistant to weathering than the adjacent dolomite strata. It tends to underlie topographically low areas and weather to rounded landforms. Finer-grained facies weather orange-brown, whereas coarser-grained beds tend to weather light gray or purple. The average thickness of the Parting Formation is about 80 feet. Contact with underlying Fremont Dolomite is a major unconformity at the Ordovician-Devonian boundary.

MDu Mississippian and Devonian rocks, undivided

Ofh Fremont Formation and Harding Sandstone, undivided (Upper and Middle Ordovician) — The Fremont Formation typically is dark to medium gray or brown gray, but locally is mottled light and dark gray. Crystalline, fetid dolomite with abundant echinoderm parts and rare dolomitized coral in a fine-grained dolomite matrix comprise most of the formation. The formation is massive, with faint, poorly preserved bedding that is 1 to 3 inches thick. Weathered outcrops have high surface roughness. It crops out only in the southwest corner of the quadrangle, where it forms a sharp ridge in a canyon on the southwest side of Kaufman Ridge. Thickness is about 50 to 70 feet. The Fremont Formation disconformably overlies the Harding Sandstone.

The Harding Sandstone consists of gray, dark-red-orange, and purple, fine- to medium-grained, well indurated, mottled quartz arenite with siliceous cement. Planar laminae are common. It weathers light gray and opaque orange-brown. Silica grains with conchoidal fractures are common. The formation has faint bedding that is 0.5 to 3 inches thick. Rare pebble-conglomerate beds interbedded with the sandstone locally include large white angular feldspar clasts up to 3 inches in diameter. This conglomerate unit was observed in a saddle on Kaufman Ridge near the south edge of the quadrangle. An opaque, white to tan quartzite breccia found on the east side of Kaufman Ridge is intensely fractured and contains angular clasts of both

dolomite and quartzite up to 6 inches in diameter. The Harding Sandstone disconformably overlies the Manitou Limestone and is about 30 to 50 feet thick.

Om Manitou Formation (Lower Ordovician) — Consists mostly of light-gray, dark- to medium-gray, and gray-brown, massive to bedded (beds up to 2 inches thick), micritic and fine-grained crystalline dolomite containing rare beds of limestone. On weathered surfaces it is light gray, chalky white, or brown. Outcrops are rough and pitted, but are not as sharp and jagged as the Leadville Limestone. It contains numerous silicified burrows with white chert stringers. Linear veins of calcite or calcite infilling along bedding planes are common locally. The Manitou Formation forms the prominent hundred-foot-high cliffs on the west side of Kaufman Ridge. Boulders up to 40 feet long have fallen from massive cliff faces in the SE $\frac{1}{4}$ NE $\frac{1}{4}$ of section 27, T. 13 S., R. 77 W. The Manitou Formation averages about 150 to 200 feet thick. The contact with the underlying Cambrian formations is disconformable (De Voto, 1971).

Dou Devonian and Ordovician rocks, undivided

€ds Dotsero Formation and Sawatch Sandstone, undivided (Upper Cambrian) — Excellent exposures of the undivided unit that includes the Dotsero Formation and underlying Sawatch Sandstone are found along the crest of Kaufman Ridge and locally on the hill slope on the western side of Kaufman Ridge. In a regional study of the Cambrian and Ordovician rocks Myrow and others (2003) divided the Dotsero Formation into three members. Two of those members, a green-brown Redcliff Member and an underlying dark-maroon Sheep Mountain Member, exist within the quadrangle. The uppermost member, the Glenwood Canyon Member, and a distinctive bed at the top of that member called the Clinetop Bed were not observed in the quadrangle.

The Red Cliff Member consists of well-sorted, planar-bedded, fine-grained quartz arenite with carbonate cement and glauconite mineralization. The Sheep Mountain Member is a reddish-purple, coarse-grained, quartz arenite with 6- to 8-inch cross-bedding. The Red Cliff Member locally contains copper mineralization in a breccia zone at the top of the unit. A shaft driven on the Dotsero and Sawatch contact in the NW $\frac{1}{4}$ NW $\frac{1}{4}$ section 35, T. 13 S., R. 77 W. also shows abundant mineralization. The Red Cliff Member is about 30 feet thick, and the Sheep Mountain Member is 8 to 13 feet thick.

The Sawatch Sandstone consists of pale pink and white, fine- to medium-grained, well-sorted, quartz arenite that weathers orangish brown. The Sawatch, Dotsero, and Manitou formations form a 60-foot-high cliff on Kaufman Ridge in the NW $\frac{1}{4}$ NE $\frac{1}{4}$ of section 35, T. 13 S., R. 77 W. The Sawatch Sandstone locally includes a white quartz-pebble conglomerate bed with $\frac{1}{4}$ inch to $\frac{3}{4}$ inch angular quartz clasts that is exposed near the same shaft described in the preceding paragraph. Thickness of the Sawatch Sandstone is variable; it is a maximum of about 30 feet thick. The contact with the underlying Proterozoic rocks is a major unconformity.

Proterozoic Crystalline Rocks

YXg Granite porphyry (Mesoproterozoic or Paleoproterozoic) — A small area along the south edge of the quadrangle and on the west flank of Kaufman Ridge is underlain by granite porphyry. The groundmass consists of potassium feldspar, quartz, plagioclase, and biotite. The potassium feldspar crystals in the groundmass are dark pink and 0.04 to 0.08 inches long. In thin section they show tartan twinning. Quartz crystals are gray, glassy, anhedral, and are slightly

smaller than the potassium feldspar crystals. Plagioclase crystals are milky white and 0.08 to 0.16 inches long. In thin section they show albite twinning and brownish alteration. Biotite occurs as aggregates of small black crystals that are 0.08 to 0.16 inches in diameter. In some thin sections minor muscovite occurs with the biotite. Larger crystals are dark-pink potassium feldspar; they are about 0.4 to 0.8 inches long. Some exhibit carlsbad twinning. No intact outcrops of granite bedrock were found in the quadrangle; it crops out only as rubbly talus on steep slopes. Clasts of pegmatite composed of quartz and potassium feldspar also occur in the talus, which suggests bodies of pegmatite may exist within areas mapped as granite.

Xb Biotite gneiss (Paleoproterozoic) – Biotite gneiss crops out along the west flank of Kaufman Ridge. It is composed of quartz, biotite, potassium feldspar, and plagioclase crystals about 0.02 to 0.08 inches in diameter. Potassium feldspar crystals are pink, anhedral, tartan-twinned, and slightly larger than the other minerals. Biotite crystals are black and have well-developed crystal faces. Quartz crystals are gray, glassy, and tend to be smaller than other minerals. Plagioclase crystals are grayish-white, and some show albite twinning. The gneiss is moderately well foliated, with the biotite forming the dark layers and potassium feldspar, quartz, and plagioclase forming the light-colored layers. Plagioclase is about twice as abundant as potassium feldspar. Rubbly talus overlies most areas mapped as biotite gneiss, but there are a few small outcrops near the southern edge of the quadrangle. Pieces of granite porphyry similar to unit YXg were also found in the talus, indicating that granite intrusions are present in unit Xb.

STRATIGRAPHY

The oldest rocks in the Antero Reservoir quadrangle are Paleoproterozoic biotite gneiss and Mesoproterozoic or Paleoproterozoic granite porphyry that crop out on Kaufman Ridge. The lower and middle Paleozoic is represented by the Sawatch, Manitou, Harding, Fremont, Parting, Dyer, and Leadville formations, which were recognized and described in the Antero Reservoir quadrangle by Johnson (1934). Later the Dotsero Formation was recognized in the area by Myrow and others (2003). These limestone, dolomite, and sandstone formations were deposited in shallow tropical seas that periodically covered much of the western United States. They are separated by unconformities that developed when the seas retreated and exposed the rocks to erosion. Later, when mineral-rich fluids migrated through the area, these unconformities were preferred pathways where minerals were deposited. For this reason a number of prospect pits on Kaufman Ridge occur at formation boundaries.

A variety of names have been applied to the Pennsylvanian and Permian rocks on the Antero Reservoir quadrangle (see, for example, Johnson, 1934; Gould, 1935; Brill, 1952; and De Voto, 1971), and these names have been applied differently by different people. For the sake of simplicity and to avoid confusion we have chosen to map the Belden, Minturn, and Maroon formations as recommended by Tweto (1949). The Minturn and Maroon formations were originally named in the Pando area (Tweto, 1949) and in the Crested Butte area (Eldridge, 1894), respectively.

To support previous Colorado Geological Survey mapping projects in the area, stratigraphic sections in the upper Minturn and lower Maroon formations were measured from Hoosier Pass to southern South Park and correlated with the section by Tweto (1949) in the Pando area (for details see Kirkham and others, 2006, 2007; and Widmann and others, 2005, 2011). This enabled the tracing of various limestone members and clastic wedges southward into the Antero Reservoir quadrangle. The rocks in the Minturn and Maroon formations undergo numerous facies changes as they are traced southwards. On the Antero Reservoir quadrangle they are more fine-grained and silty than they are in their type areas. For these reasons some revisions to the stratigraphic nomenclature of these rocks in the South Park area may be in order, but that is beyond the scope of this project. For this map we recognize one formal member of the Minturn Formation (Coffman Member) and two informal units (an upper interval and lower interval). We also map a locally present evaporite facies within the upper interval.

We also chose to map the Coffman Member as defined originally by Gould (1935), but we followed the practice of De Voto (1972) in assigning it to the Minturn Formation. De Voto (1972) and Kelly (1984) extended the Coffman Member northward to include a coarse clastic wedge in the Fairplay West quadrangle. However, previous mapping by the Colorado Geological Survey (Widmann and others, 2006, 2011) has shown that the coarse clastic wedge to the north is not contiguous with the Coffman Member in its type area on the Antero Reservoir quadrangle. They are also lithologically different, in that the Coffman to the north is much richer in quartz than the Coffman in its type area. The clastic wedge to the north also occurs lower in the section and is older than the Coffman on the Antero Reservoir and Castle Rock Gulch quadrangles (Widmann and others, 2006, 2011; Henry, 1998; Houck and others, 2004; Wallace and Keller, 2003).

Ancient mountain ranges are thought to have existed in the general vicinity of the present sites of the Front Range, the Uncompahgre Uplift, and possibly the Sawatch Range (Mallory, 1972; De Voto, 1980; De Voto and others, 1986), although the modern uplifts don't exactly match with the Pennsylvanian ones. The South Park sub-basin of the Central Colorado Basin

was sometimes covered by marine water as evidenced by the presence of marine fossils in some places. When the seawater evaporated, minerals such as gypsum and halite were deposited. When these minerals dissolve, sinkholes and other collapse structures can form. Deformation related to dissolution and/or flow of evaporite minerals may also be responsible for movement on some of the faults and folds in the quadrangle.

A small igneous stock and several associated dikes (unit Ti) intrude Pennsylvanian sedimentary rocks on the upthrown side of the Trout Creek fault. The stock and dikes are elongated parallel to the fault and probably were injected into the fault zone. Although the fault appears to form the west side of the stock, and one of the dikes appears to lie within the fault zone, cross-cutting relationships between the intrusion and fault are not well exposed. It is unclear whether the intrusion is displaced by the fault. De Voto (1971) assigned a Paleocene or Eocene age to the intrusion, whereas Scott and others (1978) and Scott (2008) suggested it perhaps was Eocene. The silica and total alkali content of the intrusion is similar to that of the andesitic extrusive rocks in unit Tva, but also to Laramide intrusions in other parts of the region. Sanidine from a sample collected from the stock (sample number A983) yielded an $^{40}\text{Ar}/^{39}\text{Ar}$ age of 60.45 ± 0.15 Ma (M.J. Kunk, 2011, written communication), confirming the intrusion cooled during the Paleocene.

Eocene, Oligocene, and Miocene volcanic and sedimentary rocks crop out along the western and northern sides of the Antero syncline and on McQuaid Butte, Hall Butte, and Mount Hall in areas underlain by the evaporite facies of the Minturn Formation. These rocks include the andesitic rocks of unit Tva, Wall Mountain Tuff, Tallahassee Creek Conglomerate, Antero Formation, Wagontongue Formation, and the Tertiary limestone of unit Tlm.

The oldest volcanic rocks in the quadrangle are in unit Tva. De Voto (1971), Scott and others (1978), and Scott (2008) correlated the andesitic rocks of unit Tva with the Buffalo Peaks Andesite. That unit was first described by Whitman Cross and S.F. Emmons (in Cross, 1883), was named by Gould (1935), and described in some detail by Sanders and others (1976). However, the age assigned to the Buffalo Peaks Andesite by these authors varied. De Voto (1971) reported that the Buffalo Peak Andesite (our unit Tva) was younger than the Wall Mountain Tuff (which he called the Agate Creek Tuff) and was older than the Tallahassee Creek Conglomerate (which he called the lower volcanic conglomerate). Scott and others (1978) and Scott (2008) assigned a much younger age to the Buffalo Peaks Andesite and indicated it is younger than the Wall Mountain Tuff, Tallahassee Creek Conglomerate, and even the Antero Formation. The only $^{40}\text{Ar}/^{39}\text{Ar}$ age available for the andesite at Buffalo Peaks is a recent but unpublished age by W.C. McIntosh (2006, written communication), which, when recalibrated using a monitor age of 28.02 Ma for the Fish Canyon Tuff (Renne and others, 1998), is 38.04 ± 0.55 Ma. This date indicates the Buffalo Peaks Andesite is older than the Wall Mountain Tuff.

A sample collected from unit Tva on McQuaid Butte during this study yielded an age of 37.84 ± 0.19 Ma (Appendix B), which also predates the Wall Mountain Tuff and is within the error margins of the age of the Buffalo Peaks Andesite. This age suggests unit Tva may be correlative with the Buffalo Peaks Andesite at its type locality. However, our new chemical data raises questions about this correlation. The four samples of andesitic rocks from unit Tva that were collected within the quadrangle plot in a tight cluster on a total alkali-silica plot (Fig. 8). They contain 5 to 6 % more total alkali and about 1 % more silica than the samples from the Buffalo Peaks Andesite that were chemically analyzed by Campbell (1994), Widmann and others (2011), and Houck and others (in preparation). Additional work is needed to discern whether the rocks in unit Tva are correlative to the Buffalo Peak Andesite at Buffalo Peaks.

During the late Eocene the Wall Mountain Tuff was erupted from a caldera that probably was located in the Sawatch Range. Sanidine from the Wall Mountain Tuff has yielded an average $^{40}\text{Ar}/^{39}\text{Ar}$ age of 36.93 ± 0.11 Ma (recalibrated from McIntosh and Chapin, 2004, using a monitor age of 28.02 Ma for the Fish Canyon Tuff). The Wall Mountain ignimbrite was thick in the topographically low areas and thinner or absent over the low hills. Erosion subsequently stripped off much of the Wall Mountain Tuff, and a new landscape was created.

The Tallahassee Creek Conglomerate was unconformably deposited on the post-Wall Mountain Tuff erosion surface. Available data within the quadrangle are inadequate to determine whether the conglomeratic unit accumulated only in paleovalleys, or whether it was sufficiently thick to cover drainage divides. Studies elsewhere in the region indicate the Tallahassee Creek Conglomerate was a widespread deposit that spread across much of southern South Park and extended southward nearly to the Arkansas River. To the south, in the Black Mountain and Cover Mountain 15-minute quadrangles, the Tallahassee Creek Conglomerate reportedly is overlain by the Tuff of Stirrup Ranch (Epis and others, 1979; Wobus and others, 1979), which has yielded an age of 36.74 ± 0.16 Ma (McIntosh and Chapin, 2004; recalibrated using a monitor age of 28.02 Ma for the Fish Canyon Tuff). However, recent field investigations raise doubts about whether the Tuff of Stirrup Ranch is an ignimbrite; it may actually consist of large blocks of Wall Mountain Tuff that are incorporated into a debris flow.

The Antero Formation accumulated in a lake or series of lakes that locally flooded an erosion surface carved across the area after deposition of the Tallahassee Creek Conglomerate. Shortly after Antero deposition initiated, a relatively thin and nonwelded ash-flow tuff (unit Tat) was erupted. This ignimbrite crops out along the northwest and west sides of the Antero syncline in the east-central part of the quadrangle. An $^{40}\text{Ar}/^{39}\text{Ar}$ age of 34.03 ± 0.09 Ma was obtained on a sample from unit Tat in the quadrangle, which is within the error of the 33.90 ± 0.10 Ma age of the Antero Tuff (McIntosh and Chapin, 2004; recalibrated using a monitor age of 28.02 Ma for the Fish Canyon Tuff; see Appendix B).

Conglomerate, sandstone, and siltstone of unit Tac were deposited sometime after the eruption of the Antero ignimbrite. As the middle and upper parts of the Antero Formation were deposited, conditions at times were favorable for the deposition of limestone (unit Tal). The Antero limestone beds within the quadrangle generally consist of impure microcrystalline limestone that locally is rich in ooids and ostracods. In some samples the ostracod carapaces are articulated and not preferentially oriented, suggestive of deposition in a fairly low-energy environment. In nearby areas some Antero limestone beds are algal in origin (Johnson, 1937b). The Antero limestones probably were deposited in or along the shorelines of shallow lakes that at times were probably enriched with silica from the volcanic tephra that fell into them.

The poorly lithified clastic rocks in the axial part of the Antero syncline are correlated with the Miocene Wagontongue Formation. Some prior workers (Johnson, 1937a; Stark and others, 1949; De Voto, 1964, 1971) subdivided the Miocene rocks into two formations on the basis of grain size. The conglomeratic strata were included in the Trump Formation and the finer-grained strata were called the Wagontongue Formation. However, Scott and others (1978) argued that the Trump was merely a coarse-grained facies of the Wagontongue, and therefore it was an unnecessary name and should be abandoned. Scott and others (1978) mapped all the Miocene sediments within the Antero syncline as the Wagontongue Formation, an approach which we adopt. The evidence of a late Miocene age for these sediments, which was summarized by De Voto (1971), comes from the fine-grained part of the formation, not the coarse-grained sediments like those within the quadrangle.

The unit herein called Tertiary limestone (unit Tlm) was previously mapped by De Voto (1971) and Scott (2008) as a limestone facies at the base of the Tallahassee Creek Conglomerate. However, the limestone may be a much younger deposit that unconformably overlies Paleozoic rocks and some or all of the Tertiary rocks. It is unlike the lacustrine limestones in the Tallahassee Creek Conglomerate immediately south of the quadrangle. Additional detailed study of unit Tlm is needed to decipher its origin and age.

During the Quaternary, melt water from glaciers or snow fields in the Mosquito Range west of the quadrangle flowed down the South Platte River, Buffalo Creek, Spring Creek, and Salt Creek, episodically depositing outwash or stream alluvium across the quadrangle. The oldest outwash in the quadrangle is in the middle Pleistocene unit Qa4 in the northeast corner of the quadrangle. Late middle and late Pleistocene outwash and alluvium is widespread in many of the valleys. During the late Pleistocene and Holocene stream alluvium, colluvium, landslide deposits, and fan deposits applied some of the final touches to the modern landscape.

Modern Spring Creek apparently moved into its current position during the Holocene. Spring Creek once flowed into Buffalo Creek via a short paleovalley in the center of the N $\frac{1}{2}$ N $\frac{1}{2}$ of section 27, T. 12 S., R. 77 W. The capture was accomplished by headward erosion of the stream in the S $\frac{1}{2}$ of section 26. The paleovalley contains deposits interpreted to be Holocene in age, which indicates the capture occurred during the Holocene.

STRUCTURAL GEOLOGY

The structural geology of the Antero Reservoir quadrangle is complex, and the relatively poor exposures complicate efforts to fully understand it. Most faults were recognized by the presence of stratigraphic discontinuities such as missing section or repeated section, by abrupt changes in strikes and dips, by the presence of aligned springs and seeps, and by linear topographic features.

Little is known about the Precambrian structures because outcrops of those rocks are limited to a small area in the southwest part of the quadrangle. Erosion carved a major unconformity across the Precambrian rocks prior to the Late Cambrian. A sequence of Upper Cambrian through Mississippi sediments were episodically deposited over the region during a time of repeated rise and fall of sea level and/or pulses of regional uplift and subsidence.

During the late Paleozoic the quadrangle was within a depositional basin called the Central Colorado Trough, which lay between the Ancestral Front Range Highland to the east and the Ancestral Uncompahgre Highland to the west. No evidence of structures active during the late Paleozoic were found within the quadrangle.

Tectonism and igneous activity associated with the Laramide orogeny began near the end of the Cretaceous and continued well into the Tertiary. It was during this time when South Park basin formed. The western side of the South Park basin coincided in part with the eastern margin of the large Sawatch uplift (Tweto, 1980). The west-vergent Elkhorn thrust fault, which placed Precambrian rocks over lower Tertiary and older rocks, formed the eastern margin of South Park basin. A series of generally north-south-trending, down-to-west, typically high-angle reverse and thrust faults developed between the Elkhorn thrust and Sawatch uplift. Several of these faults exist within the quadrangle, including the Trout Creek fault. A number of previously unknown, generally east-west-trending faults were discovered during the project. Many of the north-south-trending structures appear to terminate against the east-west faults, which may be compartmental faults. Some of the faults, or some of the deformation associated with some of the faults, may be related to evaporite deformation.

The down-to-west, ~north-south-trending Trout Creek fault zone is the largest fault system in the quadrangle. It includes several north-northwest to south-southeast-trending strands with hundreds to thousands of feet of displacement. Along cross section A-A' the Belden Formation is offset about 5,600 feet by the fault. The fault is fairly linear, which suggests it is relatively high angle, and we infer it is a reverse fault, but available data are inadequate to confidently discern whether it is normal or reverse. To the west on the Marmot Peak quadrangle the Trout Creek fault appears to be offset by the Salt Creek fault and Pony Park fault. It also appears to be offset by or merge with two cross faults near Trout Creek Pass that may be right-lateral strike-slip faults. Hanging-wall anticlines and foot-wall synclines are common along the Trout Creek fault zone, although none were recognized between the cross faults on Trout Creek Pass. Tertiary dikes and a small stock intrude into the Trout Creek fault zone in section 10, T. 13 S., R. 77 W.

Salt Creek divides the quadrangle into two structurally distinct areas. North of the creek, pre-Tertiary rocks dip chiefly to the north. South of the creek, pre-Tertiary rocks are deformed by north-northwest to south-southwest-trending faults and folds, so dips typically are to the east-northeast or west-southwest.

Major structures along and north of Salt Creek include the Salt Creek and Pony Park faults (oriented roughly east-west). The Salt Creek and Pony Park faults were recognized to the

west in the Marmot Peak quadrangle by Houck and others (in preparation). These faults probably extend into the western part of the Antero Reservoir quadrangle, but they are either completely or nearly completely concealed by surficial deposits within the quadrangle. Bedrock dips generally northward on the north side of the inferred location of the Salt Creek fault, whereas on the south side the bedrock typically dips east or west and is disrupted by faults and folds. Stratigraphic relationships in the Marmot Peak quadrangle imply that the Salt Creek fault either underwent left-lateral strike-slip movement, dip-slip movement with the south side up, or a combination of the two (Houck and others, in preparation). Stratigraphic relationships in the Marmot Peak quadrangle imply that the Pony Park fault underwent right-lateral strike-slip movement, dip-slip movement with the north side up, or oblique slip (Houck and others, in preparation).

There are three other generally east-west-trending faults north of Salt Creek; they are either south of, north of, or beneath Hall Butte. A fourth fault with similar orientation may exist beneath the valley of the South Fork of the South Platte River east of Antero Dam, but due to limited data this fault is not shown on the map.

The 285 and Bare faults, which are fairly well constrained to the north on the Garo quadrangle (Kirkham and others, 2007), probably extend southward into the quadrangle, but they are concealed by Quaternary or middle to late Tertiary deposits. On the Garo quadrangle the 285 fault is inferred to be a dip-slip fault with the east side up and approximately 1,600 to 1,800 feet of stratigraphic separation (Kirkham and others, 2007). A syncline occurs on the western (downthrown) side. The 285 fault may continue into the Antero Reservoir quadrangle to where a fault with approximately the same orientation and sense of displacement occurs on the boundary between sections 24 and 25, T. 12 S., R. 77 W. Folds in the northwestern part of the quadrangle also may be associated with the 285 fault.

The Bare fault was interpreted as a down-to-west dip-slip fault with several thousand feet of stratigraphic separation on the Garo quadrangle (Kirkham and others, 2007). It probably extends into the Antero Reservoir quadrangle beneath the Tertiary rocks and Quaternary sediments in the northeastern part of the map area, where it juxtaposes the Maroon Formation against the Minturn evaporite facies.

The prominent Kaufman Ridge structure in the southwest part of the quadrangle is a Laramide-age, faulted, west-vergent anticline that trends nearly north-south and plunges north. Proterozoic rocks crop out in the axis of the structure, and Paleozoic rocks flank it. Several down-to-west, probably high-angle reverse faults cut the rocks on the west side of the Kaufman Ridge structure and in the axis as well, and a foot-wall syncline folds strata in Chubb Park. Schmidt and others (1993) described a zone of cataclasis in Proterozoic rocks within the forelimb domain. Within the quadrangle the Proterozoic rocks in the core of the Kaufmann Ridge structure are poorly exposed.

A new fault strand was identified east of Kaufman Ridge. This down-to-west fault repeats part of the section in the Belden and lower Minturn formations. Another fault in Chubb Park omits about the same stratigraphic interval, although the sense of displacement is down-to-east.

A northeast-trending fault is needed beneath Hall Butte to account for differences in the strike and dip orientations in the evaporite facies of the Minturn Formation on either side of the concealed fault. The fault also helps to account for apparent juxtaposition of stratigraphic units within the upper interval of the Minturn Formation near Antero Reservoir. Similar rationale was

used to determine the need for an east-northeast-trending fault beneath the valley of Salt Creek between Hall Butte and Mount Hall, as well as the northwest-trending fault on the east side of Hall Butte that connects the above mentioned two faults.

Most of the above described structures probably were active during the Laramide Orogeny. The generally east-west-trending faults may be compartmental faults. Some of the faults in the quadrangle also may be associated with deformation due to dissolution and/or flow of evaporite in the Minturn Formation.

Eocene to Miocene rocks in the eastern part of the quadrangle are deformed by a major structure, the Antero syncline. The axis of the fold lies east of the quadrangle (De Voto, 1971), but the west limb of the syncline is clearly expressed in the middle to late Tertiary rocks within the quadrangle. These rocks dip generally eastward, towards the syncline axis. De Voto (1971) proposed that the syncline formed over a graben in basement rocks. An alternative explanation for the Antero syncline could invoke dissolution and/or flow of evaporite in the underlying Minturn Formation.

In the southeast part of the quadrangle the Eocene Wall Mountain Tuff and overlying Tallahassee Creek Conglomerate crop out in several blocks that are tilted in varying directions. We infer that the jostled blocks probably are bounded by faults, although no exposures of these inferred faults were observed. In contrast to the down-to-west faults that cut the upper Paleozoic rocks in the west and central parts of the quadrangle, the faults in the southeast part of the quadrangle downdrop the middle Tertiary rocks to the east, towards the axis of the Antero syncline. Some of the inferred faults in middle Tertiary rocks in the southeastern most part of the quadrangle may be related to evaporite dissolution.

Eocene rocks of unit Tva, the Wall Mountain Tuff, and Tallahassee Creek Conglomerate crop out on Hall Butte, Mount Hall, and McQuaid Butte, as well as in the low hills in the east part of the quadrangle (Fig. 13). These rocks are over 1,000 feet lower in altitude than the Eocene volcanic rocks mapped at Buffalo Peaks and 'Thunder Mountain' by Widmann and others (2011) and Houck and others (in preparation). The elevation differences may reflect deposition on an erosion surface with over 1,000 feet of relief, or the differences may be due to down-to-east dip-slip faulting or to collapse associated with dissolution of evaporite in the Minturn Formation.

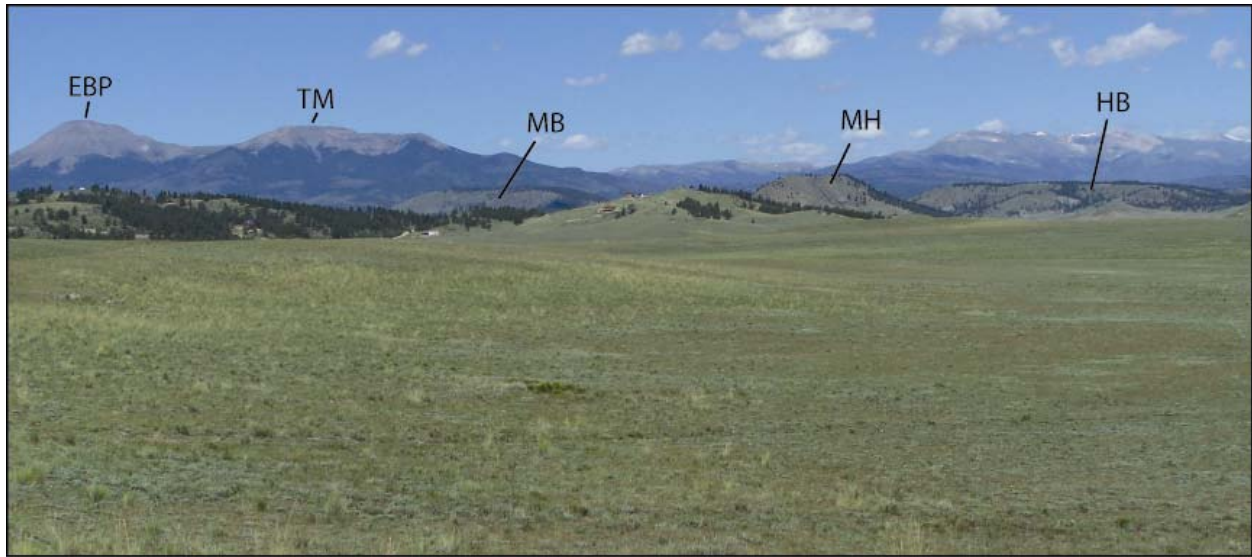


Figure 13. Overview of buttes, hills, and peaks capped by Eocene volcanic rocks in and west of the quadrangle. From right to left, they are: HB = Hall Butte, which is capped by andesitic flows of unit Tva. Remnants of the Wall Mountain Tuff and the Tallahassee Creek Conglomerate, both of which are younger than unit Tva, crop out on the lower slopes of the butte near the base of unit Tva. MH = Mount Hall, which is capped by Wall Mountain Tuff. MB = McQuaid Butte, capped by andesitic flows of unit Tva, with remnants of Wall Mountain Tuff and Tallahassee Creek Conglomerate that crop out near the base of the andesitic rocks. TM = “Thunder Mountain” and EBP = East Buffalo Peak are in the Mosquito Range and straddle the boundary of the Jones Hill and Marmot Peak quadrangles. They are capped by the Eocene Buffalo Peaks Andesite and underlying volcanic rocks (Widmann and others, 2011; Houck and others, in preparation). Low hills in the middle distance (with scattered trees and houses) are underlain by the Wall Mountain Tuff. Grassy rolling hills in foreground are underlain by the Tallahassee Creek Conglomerate. (view point location: ~UTMX: 423625, UTM Y: 4306914)

MINERAL RESOURCES

According to the on-line database of the Colorado Division of Reclamation, Mining, and Safety (<http://mining.state.co.us>) there are no active permitted mines in the quadrangle. The only mine listed in their records is a terminated permit for a sand and gravel operation in the SW $\frac{1}{4}$ SW $\frac{1}{4}$ of section 27, T. 12 S., R. 76 W. (permit no. M1978307). Schwochow (1981) reported four nonmetallic mining operations within the quadrangle, none of which are currently active or permitted. The reported operations included two sand and gravel mines near the southwest end of Antero Reservoir, a surface mine that produced crushed rock from the Wall Mountain Tuff, and the halite that was produced by evaporation of water from the salt spring at the Saltworks Ranch.

The salt works operation in the NW $\frac{1}{4}$ of section 6, T. 13 S., R. 76 W. (Fig. 14) played an important role in South Park's early history. It produced halite by evaporating water discharged from a saline spring. Refer to the chapter on Water Resources for additional information about the spring. Commercial production of halite was underway by November 1861 (Simmons, 2002). Most of the halite was used by the mills in nearby mining areas, but it was also sent to Denver and used by local ranches.

Thick deposits of gypsum and halite exist in the evaporite facies of the Minturn Formation (unit P_{me}). A small open-cut excavation (Fig. 15) and small pile of waste material and an associated disturbed area in the NW $\frac{1}{4}$ of section 27, T. 12 S., R. 77 W. suggest gypsum may have been mined or explored for there. In 1967 Wolf Ridge Mining Corporation drilled a 1,732-foot-deep hole in the N $\frac{1}{2}$ SW $\frac{1}{4}$ NE $\frac{1}{4}$ of section 27, T. 12 S., R. 76 W. in search of potassium chloride (Clement and Dolton, 1971), but apparently was unsuccessful.

The Iron Chest mine reportedly recovered zinc (sphalerite) and lead (galena) from the Minturn and Belden formations in the NE $\frac{1}{4}$ NW $\frac{1}{4}$ of section 23, T. 13 S., R. 77 W., at 38°54'37", 105°58'30", about one mile S25°W of Antero Junction, but no production was reported (McFaul and others, 2000). The shaft symbol shown on the base map of Plate 1 may mark the location of the Iron Chest mine. If this is the correct location of the mine, then our mapping suggests the shaft is in the Belden Formation.

Nelson-Moore and others (1978) described an unnamed radioactive mineral occurrence containing monazite, euxenite, and other rare-earth elements in a pegmatite in the S $\frac{1}{2}$ NE $\frac{1}{4}$ of section 22, T. 13 S. R. 77 W. This location approximately coincides with a shaft shown on the 1956 base map used for Plate 1. However, the reported location may be incorrect, because our mapping suggests the bedrock at the location is the Belden Formation, which is very unlikely to contain a pegmatite, not Proterozoic rocks, which would be more likely to host a pegmatite. No Proterozoic rocks were mapped anywhere in the S $\frac{1}{2}$ NE $\frac{1}{4}$ of section 22.

Carson Mining and Development reportedly encountered autunite mineralization containing uranium in the center of the E $\frac{1}{2}$ E $\frac{1}{2}$ of section 19, T. 13 S. R. 76 W. at 38°54'4", 105°56'11" (McFaul and others, 2000), but no evidence of mining was observed at this location in the field. However, trenches and waste piles are present in the S $\frac{1}{2}$ SE $\frac{1}{4}$ of the adjacent section 20 at locations shown on the base map as prospect pits and tailings. Nelson-Moore and others (1978) described the Carson operation as including four bulldozer trenches and eight drill holes, and they mentioned that the workings extended into section 20 and 21.

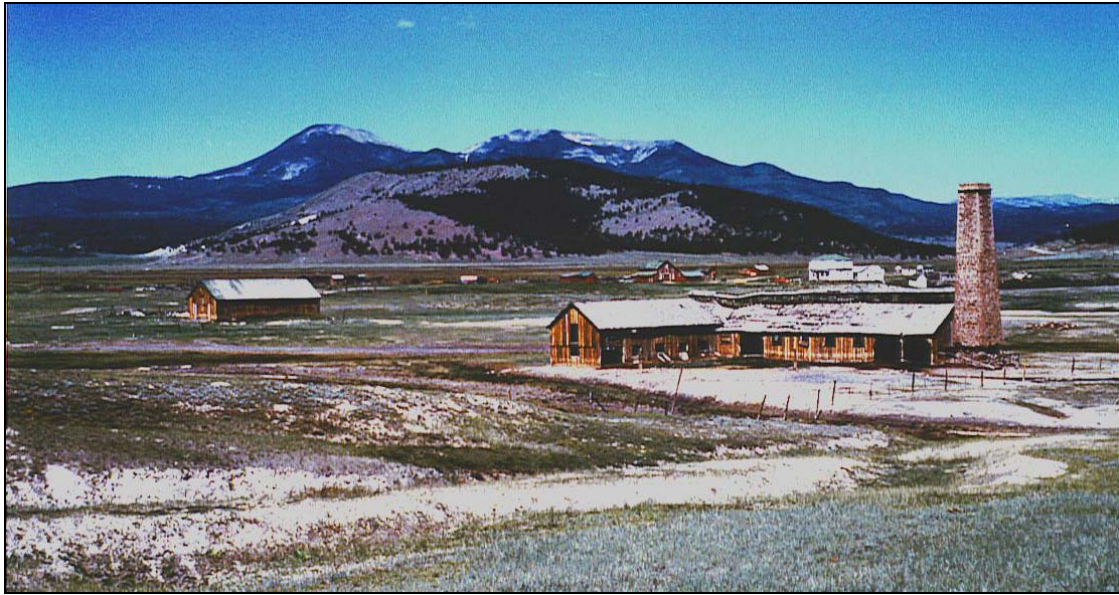


Figure 14. Historical photograph of the Salt Works ranch (courtesy of Salt Works Ranch; photograph taken in the 1960s). “L-shaped” building with tall chimney was the salt production facility, which produced halite in the 1860s to 1880s from saline water that discharged from a salt spring. Much of the building and the chimney had collapsed before the 2007 field season. The saline water currently discharges from a wood-lined hole located in the flat, snow-covered area in front of the salt works at UTMX: 418235, UTMY: 4311832. The hill behind the ranch buildings is McQuaid Butte, which is capped by andesitic flows of unit Tva that overlie the evaporite facies of the Minturn Formation. The mountains that form the skyline behind McQuaid Butte include East Buffalo Peak and an unnamed mountain to the east, both of which are capped by the Buffalo Peaks Andesite.



Figure 15. Prospect pit or small mine in an outcrop of contorted gypsum. (location: ~UTMX: 413880, UTMY: 4315030)

The outwash gravels along the South Fork of the South Platte River, Buffalo Creek, Pony Creek, Spring Creek, Salt Creek, and Trout Creek contain potentially valuable sand and gravel resources. Units Qa1, Qa2, Qa3, and Qay offer good opportunities for high-quality material. Units Qa4 and Qao also may contain sand and gravel resources.

Some of the bedrock formations also contain potential industrial mineral resources. For example, many of the hard, indurated formations may be suitable for use as aggregate or riprap. Some of the limestone beds may be sources of lime or cement.

A single oil test well, the Geary no. 1 State well, has been drilled in the quadrangle according to the records of the Colorado Oil and Gas Conservation Commission (<http://oil-gas.state.co.us/>). This well was drilled in the SW $\frac{1}{4}$ NW $\frac{1}{4}$ of section 11, T. 13 S., R. 77 W. in 1967. The well was drilled to a depth of 880 feet in Pennsylvanian sedimentary rocks and was plugged and abandoned. The well penetrated the Leadville Limestone at a depth of 770 feet (De Voto, 1971) and encountered a large volume of water at a depth of 838 feet. No additional information on the well was discovered. The location for this well may have been influenced by the gas seep in the same quarter section that was described by De Voto (1971).

WATER RESOURCES

The Antero Reservoir quadrangle is located in the headwaters region of the South Platte River watershed. The South Fork of the South Platte River, which heads near Weston Pass in the Mosquito Range, is the largest stream in the quadrangle. The South Fork flows generally southeastward, enters the quadrangle along its northern edge, and immediately drains into Antero Reservoir, the namesake of the quadrangle. Antero Dam is an earth-filled dam that was built in 1909. It is owned and operated by the Denver Water Department and used to store up to 20,000 acre-feet of water for use by their customers in the Denver metropolitan area. Recreation at the reservoir is managed by the Colorado Division of Wildlife. The reservoir was re-opened to fishing while our field work was underway, resulting in several reports in the media about the excellent fishing opportunities. According to the Denver Water Department website (<http://www.denverwater.org/recreation/antero.html>), the reservoir occupies the site of a former lake thought to be no more than 300 years old, and Green Lake lies submerged within modern Antero Reservoir.

Other perennial streams in the quadrangle include, from north to south, Buffalo Creek, Pony Creek, Spring Creek, Salt Creek, Trout Creek, and Chubb Creek all with headwaters in the Mosquito Range. Trout Creek and Chubb Creek are in the watershed of the Arkansas River, and all other streams drain into either the South Fork of the South Platte or directly into Antero Reservoir. Only intermittent streams are found in the southeastern quarter of the quadrangle. Most of these northward flowing streams empty into closed depressions before reaching Antero Reservoir.

Real-time flow data are available for perennial streams in and near the Antero Reservoir quadrangle at <http://www.dwr.state.co.us/SurfaceWater/default.aspx>. There is one stream gaging station about 1,500 feet downstream of Antero Dam (station ID PLAANTCO) that is shown on the topographic base map of the quadrangle. Another gaging station (station ID SFKANTCO) is described as being above Antero Reservoir, although a map in Kimbrough (2001) indicates the station is upstream of the quadrangle.

The only readily available annual summaries of stream discharge in and near the quadrangle are found at <http://cdss.state.co.us/DNN/Stations/tabid/74/Default.aspx>. This database includes flow data from the stream gage on the South Fork downstream of Antero Reservoir for the time period 1976 to 2006. During this time the minimum annual flow was 3,068 acre-feet, the maximum was 40,545 acre-feet, and the mean annual flow was 18,981 acre-feet. According to Kimbrough (2001) the mean annual stream flow below Antero Reservoir from 1976 to 1998 was 28.3 cubic feet per second.

Topper and others (2003) described the general ground water conditions in South Park. According to water well records held by the Colorado Division of Water Resources, most bedrock formations in the quadrangle are capable of yielding sufficient ground water for domestic purposes at depths of 100 to 400 feet, although in the higher-altitude areas in the southwest and south-central parts of the quadrangle wells have been drilled as deep as about 600 feet. Anecdotal evidence suggests the quality of ground water from the bedrock aquifers is highly variable. Wells drilled into alluvial units one, two, and three also usually yield adequate ground water for domestic purposes from relatively shallow depths.

The saline spring at the Salt Works ranch discharges from alluvium that overlies the evaporite facies of the Minturn Formation. In 1881 a group of investors reportedly sunk a thousand-feet-deep well near the spring in an effort to find and produce ground water with higher

concentrations of dissolved salt (Simmons, 2002). Eckel (1961) also described the salt works operation and provided a number of additional references for it, including Frazer (1873), who reportedly mentioned the drilling of an artesian well there in 1869. According to Eckel, the salt was recovered from a group of springs, and he described the site as a locality for halite.

The only chemical analysis of the spring water that we found during a cursory search was by George and others (1920). They reported that the salt works spring was flowing at 5 to 6 gallons per minute, had a temperature of 9.5° C, and had a total dissolved solids concentration of 30,193 milligram/liter (mg/L), including 9,513 mg/L of sodium, 15,472 mg/L of chloride, 1,074 mg/L of calcium, 2,700 mg/L of sulfate, and 900 mg/L of potassium. The chemistry of the spring water supports our hypothesis that halite, gypsum, and perhaps sylvite may be dissolving from the evaporite facies of the Minturn Formation in the subsurface. Currently, water discharges from a wood-lined hole near the east end of the old salt works facility at 418235 m E, 4311832 m N. It is unclear at this time whether the water is from the spring, the reported wells, or a combination thereof.

Another salt spring within the quadrangle exists in the NW ¼ of section 24, T. 12 S., R. 77 W. It is adjacent to Highway 285 and is labeled a salt spring on the U.S.G.S. topographic base map.

GEOLOGIC HAZARDS

The primary geologic hazards and geotechnical constraints in the Antero Reservoir quadrangle include flooding, debris flows, sinkholes, subsidence, and rockfall. Landslides, problematic soils, and earthquakes also pose potential threats. Areas underlain by alluvial unit one (Qa1), alluvium and colluvium (unit Qac), and fan deposits (unit Qf) are prone to water flooding. Debris flows, mudflows, and sheet flooding may affect areas mapped as fan deposits (unit Qf), alluvium and colluvium (unit Qac), and colluvium (unit Qc). Rockfall is a hazard below cliffs of hard, indurated rock.

Sinkholes and subsidence are hazards in areas underlain by the evaporite facies of the Minturn Formation, perhaps even in areas where those rocks are overlain by younger deposits. More than 100 sinkholes were mapped in the quadrangle, and several large subsidence depressions were identified. A cluster of sinkholes in the valley of Salt Creek are shown in Figure 16. The subsidence depressions are as much as one-half mile long, one-quarter mile wide, and about ten feet deep. If the Antero syncline formed in response to subsidence into evaporite karst, then many hundreds of feet of vertical collapse may have occurred in the past, probably over a very long period of time.



Figure 16. Cluster of sinkholes and karst topography on the valley floor of Salt Creek near the center of the E ½ of section 2, T. 13 S., R. 77 W. (~center of sinkhole cluster at UTMX: 416080, UTM Y: 4311590). Individual sinkholes range from about 20 to 110 feet in diameter. View looking north.

A few small landslides were mapped in the quadrangle. Some are on the flanks of McQuaid Butte and Hall Butte. Others were recognized in the hills held up by the middle Tertiary rocks in the southeast part of the map area and in the Minturn Formation near the northwest corner of the quadrangle. No evidence of recent activity was noted in these landslides,

but they were not examined carefully while in the field. Human activities, including excavations and earth fills on slopes and changes to the hydrologic environment from irrigation, septic systems, and water impoundments and diversions, can contribute to slope failure. Future landsliding may not be restricted only to areas mapped as landslide deposits.

Soils in areas underlain by the evaporite facies of the Minturn Formation, as well as areas containing surficial deposits derived from the evaporite facies, may have corrosive and alkali properties that are deleterious to concrete and metal. Fine-grained sediments that were rapidly deposited in fan environments and on colluvial slopes may be prone to hydrocompaction and piping. Such sediments may be found in units Qf, Qc, and Qac.

No evidence of late Quaternary faults was detected during the project, but earthquakes due to rupture of nearby faults, like those at Spinney Mountain (Shaffer and Williamson, 1986) or in the upper Arkansas Valley (Ostenaa and others, 1981; Lettis and others, 1996), could cause moderately strong ground motion in the quadrangle. A random or “floating” earthquake along a fault that is deep in the crust and does not rupture the ground surface also could generate moderately strong ground motion. To account for these types of earthquakes, structures should at least be designed and built to the standards of the current International Building Code or other appropriate building code. Site-specific seismic hazard studies should be conducted for critical structures. Earthquakes can also trigger secondary effects, such as liquefaction, rockfall, and landslides, which potentially can cause great damage.

ACKNOWLEDGMENTS

This geologic mapping project was funded jointly by the Colorado Geological Survey and U.S. Geological Survey through the STATEMAP component of the National Cooperative Geologic Mapping Program, Award number 07HQAG0083. The State of Colorado provided funding through the Department of Natural Resources Severance Tax Operational Fund, which is derived from the production of gas, oil, and minerals.

Jim Shannon and Jim Burnell described the thin sections from the igneous rocks. Vince Matthews conducted a field review of the mapping project. The map and report benefited from the review comments of Bruce Bryant, Chuck Kluth, and Cal Ruleman. Caitlin Bernier and David Barnett, with Pangaea Cartographic, prepared the digital geologic map for publication. Cartographic work for Figures 1 and 2 was performed by Larry Scott. Jeremy Webb of the Denver Waldorf School helped with data entry.

Numerous landowners and property managers or employees gave permission to conduct field work on their land and oftentimes provided valuable historic or logistical information. They include Tag Fanning with the Salt Works Ranch, John Penalver with the Ranch of the Rockies subdivision, Susan Steele-Weir, Amy Turney, Eric Hibbs, and William George with the Denver Water Department, Cliff Piper with the Sipal Ranch, and Debbie and Paul Gentry with the Campground of the Rockies Association. We are especially grateful to Mr. Fanning, who allowed us to stay in a cabin at the Saltworks Ranch while we conducted field work, and also provided us with the historical photograph of the ranch used in Figure 14.

This publication is dedicated to Alyssa D. Heberton-Morimoto, our field assistant who was tragically murdered while conducting field work during the project. We also dedicate our publication to Richard H. De Voto, who was the author of many published reports and papers on the Tertiary and Paleozoic rocks in South Park, because he passed away while our publication was in preparation.

REFERENCES CITED

- Birkeland, P.W., 1999, Soils and geomorphology, 3rd edition: New York, Oxford University Press, 430 p.
- Brill, K.G., Jr., 1952, Stratigraphy in the Permo-Pennsylvanian zeugogeosyncline of Colorado and northern New Mexico: Geological Society of America Bulletin, v. 63, no. 8, p., 809-880.
- Brown, G.F., 1940, Late Tertiary sediments in South Park, Colorado: Evanston, Illinois, Northwestern University, M.S. thesis, 43 p.
- Campbell, S.K., 1994, A geochemical and strontium isotopic investigation of Laramide and younger igneous rocks in central Colorado, with emphasis on the petrogenesis of the Thirtynine Mile volcanic field: Tallahassee, Florida State University, Ph.D. thesis, 614 p.
- Clement, J.H., and Dolton, G.L., 1970, A chronicle of exploration in South Park basin, Park County, Colorado: The Mountain Geologist, v. 7, no. 3, p. 205-216.
- Cross, W., 1883, On hypersthene-andesite and on triclinic pyroxene in augitic rocks, with a Geological sketch of Buffalo Peaks, Colorado, by S.F. Emmons: U.S. Geological Survey, Bulletin 1, 42 p.
- De Voto, R.H., 1964, Stratigraphy and structure of Tertiary rocks in southwestern South Park: The Mountain Geologist, v. 1, no. 3, p. 117-126.
- De Voto, R.H., 1971, Geologic history of South Park and geology of the Antero Reservoir quadrangle, Colorado: Quarterly of the Colorado School of Mines, v. 66, no. 4, 90 p., scale 1:62,500.
- De Voto, R. H., 1972, Pennsylvanian and Permian stratigraphy and tectonism in central Colorado: Colorado School of Mines Quarterly, v. 67, no. 4, p. 139-185.
- De Voto, R.H., 1980, Pennsylvanian stratigraphy and history of Colorado, in Kent, H.C., and Porter, K.W., eds., Colorado geology: Rocky Mountain Association of Geologists, p. 71-101.
- De Voto, R.H., Bartleson, B.L., Schenk, C.J., and Waechter, N.B., 1986, Late Paleozoic stratigraphy and syndepositional tectonism, northwestern Colorado, in Stone, D.S., New interpretations in northwest Colorado geology: Rocky Mountain Association of Geologists, p.37-49.
- Eckel, E.B., 1961, Minerals of Colorado; 100-year record: U.S. Geological Survey Bulletin 1114, 399 p.
- Eldridge, G. H., 1894, United States Geological Survey Atlas, Anthracite-Crested Butte Folio #9, 10 p.
- Epis, R.C., Wobus, R.A., and Scott, G.R., 1979, Geologic map of the Black Mountain quadrangle, Fremont and Park Counties, Colorado: U.S. Geological Survey, Geologic Quadrangle Map GQ-1195, scale 1:62,500.
- Folk, R. L., 1980, Petrology of sedimentary rocks: Austin, Texas, Hemphill Publishing Company, 182 p.
- Folk, R.L., and Ward, W.C., 1957, Brazos River bar; A study in the significance of grain size parameters: Journal of Sedimentary Petrology, v. 27, p. 3-26.
- Frazer, P., Jr., 1873, Mines and minerals of Colorado [and New Mexico]: Hayden Survey, 3rd Annual Report of the U.S. Geological Survey with Territories Embracing Colorado and New Mexico, p. 201-228.
- George, R.D., Curtis, H.A., Lester, O.C., Crook, J.K., Yeo, J.B., and others, 1920, Mineral waters of Colorado: Colorado Geological Survey Bulletin 11, 474 p.
- Gould, D. B., 1935, Stratigraphy and structure of Pennsylvanian and Permian rocks in Salt Creek area, Mosquito Range, Colorado: American Association of Petroleum Geologists Bulletin, v. 19, p. 971-1009.
- Henry, T. W., 1998, The brachiopod *Antiquatonia coloradoensis* (Girty) from the Upper Morrowan and Atokan (Lower Middle Pennsylvanian) of the United States: United States Geological Survey Professional Paper 1588, 32 p.
- Hilgard, E.W., 1892, A report on the relations of soil to climate: U.S. Department of Agriculture Weather Bureau Bulletin 3, 59 p.

- Houck, K., Fleming, J., Guerrero, R., Heimink, N., Heberton, A., Itano, W., Titus, A., and Barrick, J., 2004, Paleontology of the Bassam Park fossil beds (Pennsylvanian), San Isabel National Forest, Colorado: Geological Society of America Abstracts with Programs, v. 36, no. 5, p. 413.
- Houck, K.J., Funk, J., Carroll, C.J., Kirkham, R.M., and Heberton-Morimoto, A.D., in preparation, Marmot Peak quadrangle geologic map, Chaffee and Park Counties, Colorado: Colorado Geological Survey, scale 1:24,000.
- Ingram, R.L., 1989, Grain-size scale used by American geologists, *in* Dutro, J.T., Jr., Dietrich, R.V., and Foose, R.M., eds., AGI data sheets for geology in the field, laboratory, and office: Alexandria, VA, American Geological Institute, Data Sheet 29.1.
- Jackson, J.A., ed., 1997, Glossary of geology, 4th ed.: Alexandria, Va., American Geological Institute, 769 p.
- Johnson, J. H., 1934, A coprolite horizon in the Pennsylvanian of Chaffee and Park Counties, Colorado: *Journal of Paleontology*, v. 8, no. 4, p. 477-479.
- Johnson, J.H., 1937a, Tertiary depositions of South Park, Colorado, with a description of Oligocene algal limestones: Boulder, University of Colorado, Ph.D. dissertation, 68 p.
- Johnson, J.H., 1937b, Algae and algal limestone from the Oligocene of South Park, Colorado: *Geological Society of America Bulletin*, v. 48, p. 1227-1236.
- Johnson, J.H., 1940, Lime-secreting algae and algal limestones from the Pennsylvanian of central Colorado: *Geological Society of America Bulletin*, v. 51, p.571-596.
- Keller, J.W., McCalpin, J.P., and Lowry, B.W., 2004, Geologic map of the Buena Vista East quadrangle, Chaffee County, Colorado: Colorado Geological Survey Open-File Report 04-4, scale 1:24,000.
- Kelly, K. E., 1984, Stratigraphy and sedimentology of the Pennsylvanian Coffman Member of the Minturn Formation and Belden Formation, Mosquito Range, Colorado: Colorado School of Mines unpublished M. S. thesis, 107 p.
- Kimbrough, R.A., 2001, Review and analysis of available streamflow and water-quality data for Park County, Colorado, 1962-98: U.S. Geological Survey Water Resources Investigations Report 01-4034, 66 p.
- Kirkham, R.M., Keller, J.W., Houck, K.J., and Lindsay, N.R., 2006, Geologic map of the Fairplay East quadrangle, Park County, Colorado: Colorado Geological Survey Open-File Report 06-9, scale 1:24,000.
- Kirkham, R.M., Houck, K.J., Lindsay, N.R., and Keller, S.M., 2007, Geologic map of the Garo quadrangle, Park County, Colorado: Colorado Geological Survey Open-File Report 07-6, scale 1:24,000.
- Le Bas, M.J., LeMaitre, R.W., Streckeisen, A.I., and Zanettin, B., 1986, A chemical classification of volcanic rocks based upon the total alkali-silica diagram: *Journal of Petrology*, v. 27, p. 747-750.
- Lettis, W., Noller, J., Wong, I., Ake, J., Vetter, U., and LaForge, R., 1996, Draft report, Seismotectonic evaluation; Colorado River storage project-Crystal, Morrow Point, Blue Mesa dams; Smith Fork project-Crawford dam, west-central Colorado: report prepared by William Lettis & Associates, Inc., Woodward-Clyde Federal Services, and Seismotectonics and Geophysical Group of the U.S. Bureau of Reclamation for the U.S. Bureau of Reclamation in Denver, Colorado, 177 p.
- Lozano, E., 1965, Geology of the southwestern Garo area, South Park, Park County, Colorado: Golden, Colorado School of Mines, M.S. thesis T-1057, 206 p.
- Machette, M.N., 1985, Calcic soils of the southwestern United States, *in* Weide, D.L., ed., Soils and Quaternary geology of the southwestern United States: Geological Society of America Special Paper 203, p. 1-21.
- Mallory, W. W., 1972, Pennsylvanian arkose and the Ancestral Rocky Mountains, *in* Mallory, W. W., ed., Geologic atlas of the Rocky Mountain region: Rocky Mountain Association of Geologists, p. 131-132.

- Martinson, D.G., Pisias, N.G., Hays, J.D., Imbrie, J., Moore, T.C., Jr., and Shackleton, N.J., 1987, Age dating and the orbital theory of the ice ages; Development of a high-resolution 0 to 300,000-year chronostratigraphy: *Quaternary Research*, V. 27, P. 1-29.
- McFaul, E.J., Mason, G.T., Jr., Ferguson, W.B., and Lipin, B.R., 2000, U.S. Geological Survey mineral databases—MRDS and MAS/MILS: U.S. Geological Survey Digital Data Series DDS-52.
- McCalpin, J.P., and Shannon, J.R., 2005, Geologic map of the Buena Vista West quadrangle, Chaffee County Colorado: Colorado Geological Survey Open-File Report 05-8, scale 1:24,000.
- McIntosh, W.C., and Chapin, C.E., 2004, Geochronology of the central Colorado volcanic field, *in* Cather, S.M., McIntosh, W.C., and Kelley, S.A., eds., *Tectonics, geochronology, and volcanism in the southern Rocky Mountains and Rio Grande rift*: New Mexico Bureau of Geology and Mineral Resources Bulletin 160, p. 205-237.
- Myrow, P. M., Taylor, J. F., Miller, J. F., Ethington, R. L., Ripperdan, R. L., and Allen, J., 2003, Fallen arches: Dispelling myths concerning Cambrian and Ordovician paleogeography of the Rocky Mountain region: *Geological Society of America Bulletin*, v. 115, no. 6, p. 695-713.
- Nelson-Moore, J.L., Collins, D.B., and Hornbaker, A.L., 1978, Radioactive mineral occurrences of Colorado: Colorado Geological Survey Bulletin 40, 1054 p.
- Ostenaa, D.A., Losh, S.L., and Nelson, A.R., 1981, Evidence for recurrent late Quaternary faulting, Sawatch fault, upper Arkansas Valley, Colorado, *in* Junge, J.R., ed., *Colorado tectonics, seismicity, and earthquake hazards*: Proceedings and field trip guide: Colorado Geological Survey Special Publication 19, p. 27-29.
- Renne, P.R., Swisher, C.C., Deino, A.L., Karner, D.B., Owens, T.L., and Depaolo, D.J., 1998, Intercalibration of standards: absolute ages and uncertainty in $^{40}\text{Ar}/^{39}\text{Ar}$ dating: *Chemical Geology*, v. 145, p. 117-152.
- Ruleman, C.A., and Bohannon, R.G., 2008, Geologic map of the Elkhorn quadrangle, Park County, Colorado: U.S. Geological Survey, Scientific Investigations Series Map 3043, scale 1:24,000.
- Sanders, G.F., Jr., Scott, G.R., and Naeser, C.W., 1976, The Buffalo Peaks Andesite of central Colorado: U.S. Geological Survey, Bulletin 1405-F, p. F1-F8.
- Schmidt, C.J., Genovese, P.W., and Chase, R.B., 1993, Role of basement fabric and cover-rock lithology on the geometry and kinematics of twelve folds in the Rocky Mountain foreland, *in* Schmidt, C.J., Chase, R.B., and Erslev, E.A., eds., *Laramide basement deformation in the Rocky Mountain foreland of the western United States*: Geological Society of America Special Paper 280, p. 1-44.
- Schwochow, S.D., 1981, Inventory of nonmetallic mining and processing operations in Colorado: Colorado Geological Survey Map Series 17, 39 p.
- Scott, G.R., 1975, Reconnaissance geologic map of the Buena Vista quadrangle, Chaffee and Park Counties, Colorado: U.S. Geological Survey Miscellaneous Field Studies Map MF-657.
- Scott, G.R., 2008, Reconnaissance geologic map of the Antero Reservoir quadrangle, Chaffee and Park Counties, Colorado: U.S. Geological Survey, unpublished legacy map.
- Scott, G.R., Taylor, R.B., Epis, R.C., and Wobus, R.A., 1978, Geologic map of the Pueblo 1° x 2° quadrangle, south-central Colorado: U.S. Geological Survey Miscellaneous Investigation Series I-1022, scale 1:250,000.
- Shaffer, M.E., and Williamson, J.V., 1986, Seismic evaluation of Spinney Mountain dam, *in* Rogers, W.P., and Kirkham, R.M., eds., *Contributions to Colorado tectonics and seismicity--A 1986 update*: Colorado Geological Survey Special Publication 28, p. 104-121.
- Simmons, V.M., 2002, Bayou salado-The story of South Park: Boulder, Colorado, University Press of Colorado, 275 p.
- Stark, J.T., Johnson, J.H., Behre, C.H., Jr., Powers, W.E., Howland, A.L., Gould, D.B., and others, 1949, Geology and origin of South Park, Colorado: Geological Society of America Memoir 33, 188 p.

- Topper, R., Spray, K.L., Bellis, W.H., Hamilton, J.L., and Barkmann, P.E., 2003, Ground water atlas of Colorado: Colorado Geological Survey Special Publication 53, 210 p.
- Tweto, O., 1949, Stratigraphy of the Pando area, Eagle County, Colorado: Colorado Scientific Society Proceedings, v. 15, p. 149-235.
- Tweto, O., 1974a, Geology of the Mount Lincoln 15-minute quadrangle, Eagle, Lake, Park, and Summit Counties, Colorado: U.S. Geological Survey Miscellaneous Field Studies Map MF-556, scale 1:62,500.
- Tweto, O., 1974b, Reconnaissance geologic map of the Fairplay West, Mount Sherman, South Peak, and Jones Hill 7 ½ minute quadrangles, Park, Lake, and Chaffee Counties, Colorado: U.S. Geological Survey Miscellaneous Field Studies Map MF-555, scale 1:62,500.
- Tweto, O., 1979, compiler, Geologic map of Colorado: U.S. Geological Survey, scale 1:500,000.
- Tweto, O., 1980, Summary of Laramide orogeny in Colorado, *in* Kent, H.C., and Porter, K.W., eds., Colorado Geology: Denver, Colorado, Rocky Mountain Association of Geologists, p. 129-134.
- Tweto, O., and Lovering, T.S., 1977, Geology of the Minturn 15-minute quadrangle, Eagle and Summit Counties, Colorado: U.S. Geological Survey Professional Paper 956, 96 p.
- Wallace, C.A., and Keller, J.W., 2003, Geologic map of the Castle Rock Gulch quadrangle, Chaffee and Park Counties, Colorado: Colorado Geological Survey Open-File Report 01-1, scale 1:24,000.
- Widmann, B.L., Bartos, P.J., Madole, R.F., Barbá, K.E., and Moll, M.E., 2004, Geologic map of the Alma quadrangle, Park and Summit Counties, Colorado: Colorado Geological Survey Open-File Report 04-3, scale 1:24,000.
- Widmann, B.L., Kirkham, R.M., Houck, K.J., and Lindsay, N.L., 2006, Geologic map of the Fairplay West quadrangle, Park County, Colorado: Colorado Geological Survey Open-File Report 06-7, scale 1:24,000.
- Widmann, B.L., Kirkham, R.M., Houck, K.J., and Lindsay, N.L., 2011, Jones Hill quadrangle geologic map, Park County, Colorado: Colorado Geological Survey, scale 1:24,000.
- Widmann, B.L., Kirkham, R.M., Keller, J.W., Poppert, J.T., and Price, J.B., 2005, Geologic map of the Como quadrangle, Park County, Colorado: Colorado Geological Survey Open-File Report 05-4, scale 1:24,000.
- Wobus, R.A., Epis, R.C., and Scott, G.R., 1979, Geologic map of the Cover Mountain quadrangle, Fremont, Park, and Teller Counties, Colorado: U.S. Geological Survey, Geologic Quadrangle Map GQ-1179, scale 1:62,500.
- Wyant, D.G., and Barker, F., 1976, Geologic map of the Milligan Lakes quadrangle, Park County, Colorado: U.S. Geological Survey Geologic Quadrangle Map GQ-1343, scale 1:24,000.

APPENDIX A. Whole-rock major-element geochemical analyses of samples from the Antero Reservoir quadrangle. All analyses were performed by ALS Chemex using the XRF method. Sample locations (in NAD 83) are listed below the table. Sample locations also are shown on the geologic map.

ID #	Unit*	SiO ₂	Al ₂ O ₃	Fe ₂ O ₃	CaO	MgO	Na ₂ O	K ₂ O	Cr ₂ O ₃	TiO ₂	MnO	P ₂ O ₅	SrO	BaO	LOI [§]	Total
		wt %	wt %	wt %	wt %	wt %	wt %	wt %	wt %	wt %	wt %	wt %	wt %	wt %	wt %	wt %
A129	Tva	59.65	16.29	6.28	5.07	2.54	2.86	2.59	0.01	0.81	0.08	0.30	0.13	0.08	3.15	99.83
A133	Tva	61.70	16.50	6.09	4.87	1.99	3.21	3.26	<0.01	0.74	0.09	0.27	0.07	0.12	0.91	99.82
A137	Tva	61.02	16.56	6.22	4.70	1.83	3.14	3.30	<0.01	0.75	0.07	0.27	0.07	0.11	1.80	99.85
A146	Tva	61.49	16.45	6.14	4.96	1.75	3.20	3.29	<0.01	0.77	0.07	0.28	0.07	0.12	1.26	99.84
A142	Twm	70.78	14.32	1.91	1.40	0.30	3.47	5.30	<0.01	0.41	0.04	0.08	0.03	0.20	1.53	99.76
A166	Twm	69.27	15.36	2.17	1.46	0.49	3.76	5.82	<0.01	0.49	0.05	0.06	0.03	0.20	0.60	99.77
A348	Twm	67.29	15.47	2.18	2.03	0.51	3.29	6.03	<0.01	0.46	0.04	0.10	0.03	0.22	2.11	99.76
A217	Tat	62.10	15.74	4.25	3.97	1.39	2.76	2.49	<0.01	0.62	0.05	0.23	0.17	0.09	5.02	98.89
A236	Tat	63.41	15.28	4.45	4.16	1.60	2.93	2.68	<0.01	0.61	0.07	0.24	0.14	0.09	4.10	99.76
A288	Tat	65.66	14.91	4.27	3.35	1.23	2.80	2.70	<0.01	0.64	0.04	0.11	0.10	0.12	3.86	99.79
A320	Ttc	67.01	14.67	4.94	3.13	0.71	2.91	3.60	<0.01	0.76	0.03	0.28	0.06	0.10	1.62	99.81
A324	Ttc	58.72	17.37	6.66	5.08	1.54	3.60	3.74	<0.01	0.95	0.05	0.41	0.08	0.09	1.48	99.78
A391	Tt	70.84	13.37	2.37	0.66	0.73	1.93	6.24	<0.01	0.43	0.05	0.10	0.01	0.14	3.00	99.87
A983	Ti	61.07	16.66	5.99	4.94	2.23	3.20	3.32	0.01	0.76	0.08	0.28	0.07	0.11	1.09	99.82

* Refer to map or to section on Description of Map Units for an explanation of the unit symbols

§ LOI = loss on ignition

Sample Locations

A129: 414065 m E; 4313977 m N
A133: 415219 m E; 4313058 m N
A137: 414138 m E; 4313345 m N
A142: 415790 m E; 4313548 m N
A146: 418428 m E; 4313285 m N
A166: 418910 m E; 4311125 m N
A217: 423627 m E; 4314471 m N
A236: 421878 m E; 4312668 m N
A288: 423593 m E; 4316690 m N
A320: 421766 m E; 4309949 m N
A324: 421611 m E; 4310164 m N
A348: 420377 m E; 4308473 m N
A391: 423772 m E; 4304347 m N
A983: 414538 m E; 4310236 m N

$^{40}\text{Ar}/^{39}\text{Ar}$ Geochronology Results from the Antero Reservoir Quadrangle

By

Lisa Peters

AUGUST 13, 2009

Prepared for

Bob Kirkham
5253 County Road 1 South
Alamosa, CO 81101

NEW MEXICO
GEOCHRONOLOGY RESEARCH LABORATORY
(NMGRL)

CO-DIRECTORS

DR. MATTHEW T. HEIZLER

DR. WILLIAM C. McINTOSH

LABORATORY TECHNICIAN

LISA PETERS

Internal Report #: NMGRL-IR-635

Introduction

Three Tertiary volcanic flows from the Antero Reservoir quadrangle in South Park, Colorado were submitted by Robert Kirkham as part of the state map program. The separated phase and data is summarized below.

Table 1. Brief summary of results.

Sample	Phase	Age $\pm 2\sigma$ (Ma)	Comments
A217	Sanidine	34.03 \pm 0.09	Well-behaved
A320	Biotite	37.07 \pm 0.20	Somewhat disturbed
A129	Hornblende	37.84 \pm 0.19	Somewhat disturbed

⁴⁰Ar/³⁹Ar Analytical Methods and Results

Samples were initially prepared by crushing, sieving and then washing away clay-sized material. The sanidine was then cleaned in hydrofluoric acid, rinsed in distilled water and then separated with heavy liquid. Hornblende and biotite was separated with a magnetic separator, heavy liquid and hand picking. The mineral separates and monitors (Fish Canyon tuff sanidine, 28.02, Renne et al., 1998) were loaded into aluminum discs and irradiated for 7 hours at the Nuclear Science Center in College Station, Texas.

The sanidine and monitors were analyzed by the single crystal laser fusion method. The biotite and hornblende were analyzed with the furnace incremental heating age spectrum method. Abbreviated analytical methods for the dated sample are given in Table 2, and details of the overall operation of the New Mexico Geochronology Research Laboratory is provided in the Appendix. The age results are summarized in Tables 1 and 2 and the argon isotopic data are given in Tables 3 and 4.

A217 Weighted Mean Age=34.03±0.09 Ma n/n_{total}=16/17 MSWD=3.13

A217 sanidine yielded a near-Gaussian distribution (Figure 1). Sixteen of the seventeen analyzed crystals were used to calculate the weighted mean age of 34.03±0.09 Ma. The eliminated crystal is a plagioclase crystal ~6 Ma older than the other analyzed crystals. The radiogenic yields of the sanidine are consistently high, between 97.5% and 100.2%. K/Ca values of the sanidine range from 33.5 to 340.0.

A-320 Weighted Mean Age=37.07±0.20 Ma n/n_{total}=4/12 MSWD=4.37

A320 biotite yielded a disturbed age spectrum with the apparent ages stair-stepping downward over the majority of the age spectrum (Figure 2a). The apparent ages range from 32.53 Ma to 36.27 Ma. A weighted mean age of 37.07±0.20 Ma is calculated from the flattest mid-portion of the age spectrum. Radiogenic yields increase rapidly over the initial 12.9% of the age spectrum to 93.0% and remain high over the remainder of the age spectrum. K/Ca values are somewhat oscillatory initially increasing from 3.5 to 16.2 over 15.1% of the ³⁹Ar released, followed by a drop to 3.6 and then another rise to 93.0. Inverse isochron analysis of steps A-L yield an isochron age of 37.08±0.39 Ma with a ⁴⁰Ar/³⁶Ar ratio of 295.8±12.4, within error of the atmospheric ratio of 295.5 (Figure 2b).

A129 Weighted Mean Age=37.84±0.19 Ma n/n_{total}=2/9 MSWD=0.87

A129 yielded a somewhat disturbed, low-resolution age spectrum (Figure 3a). The initial 5.9% of the ³⁹Ar released yields in general low precision, young apparent ages. Two concordant steps that contain 80.8% of the ³⁹Ar released follow this. A weighted mean age of 37.84±0.19 Ma is calculated from these steps. The final two steps reveal a decrease in apparent age to 18.05 Ma. The radiogenic yields increase from 1.5% to 91.5% over 86.7% of the age spectrum. This is followed by a decrease to 73.8% radiogenic over the final two steps. Following a spike to 0.32 the K/Ca values remain fairly constant between ~0.1-0.2 over the majority of the age spectrum. Steps A-G were evaluated on an inverse isochron and found to have a ⁴⁰Ar/³⁶Ar intercept of 291.4±9.7 and an isochron age of 37.84±0.19 Ma (Figure 3b).

Discussion

We assign the weighted mean age calculated from sixteen of the seventeen analyzed A217 crystals (34.03 ± 0.09 Ma) and the weighted mean ages calculated from the age spectra analyses of A320 (37.07 ± 0.20 Ma) and A129 (37.84 ± 0.19 Ma) as the eruption ages of these volcanic flows. The sanidine from A217 provides very precise, reliable data. We note that this age is within error of the age of the Antero Tuff, 33.98 ± 0.10 Ma (recalibrated to Renne et al, 1998, McIntosh and Chapin, 2004). The age spectra for A320 biotite and A129 hornblende provide somewhat less precise, reliable data. The disturbed stair-stepping age spectrum of A320 biotite is suggestive of slight alteration and possible ^{39}Ar recoil (low K alteration phases resulting in a redistribution of ^{39}Ar created at the reactor) or excess Ar. We note however that the integrated age (37.03 ± 0.16 Ma) agrees within error to the calculated weighted mean age (37.07 ± 0.20 Ma) so the affect of either recoil and/or excess Ar has been minimal and the assigned age is probably fairly accurate. The low apparent ages revealed in the last two heating steps of A129 hornblende age spectrum is possibly the result of low K, high temperature degassing inclusions and ^{39}Ar recoil into those inclusions. Once again, with only 13.3% of the age spectrum affected by these anomalously young ages, we feel fairly confident that the assigned age of 37.84 ± 0.19 Ma provides a reliable eruption age for this volcanic flow.

References Cited

- McIntosh, W.C., and Chapin, C.E., 2004, Geochronology of the central Colorado volcanic field: New Mexico Bureau of Geology & Mineral Resources Bulletin 160, p. 205-238.
- Renne, P.R., C.C. Swisher, A.L. Deino, D.B. Karner, T.L. Owens and D.J. Depaolo, 1998, Intercalibration of standards: absolute ages and uncertainties in $^{40}\text{Ar}/^{39}\text{Ar}$ dating. *Chem. Geol.*, v. 145, p.117-152.
- Steiger, R.H., and Jäger, E., 1977. Subcommittee on geochronology: Convention on the use of decay constants in geo- and cosmochemistry. *Earth and Planet. Sci. Lett.*, 36, 359-362.
- Taylor, J.R., 1982. *An Introduction to Error Analysis: The Study of Uncertainties in Physical Measurements.* Univ. Sci. Books, Mill Valley, Calif., 270 p.

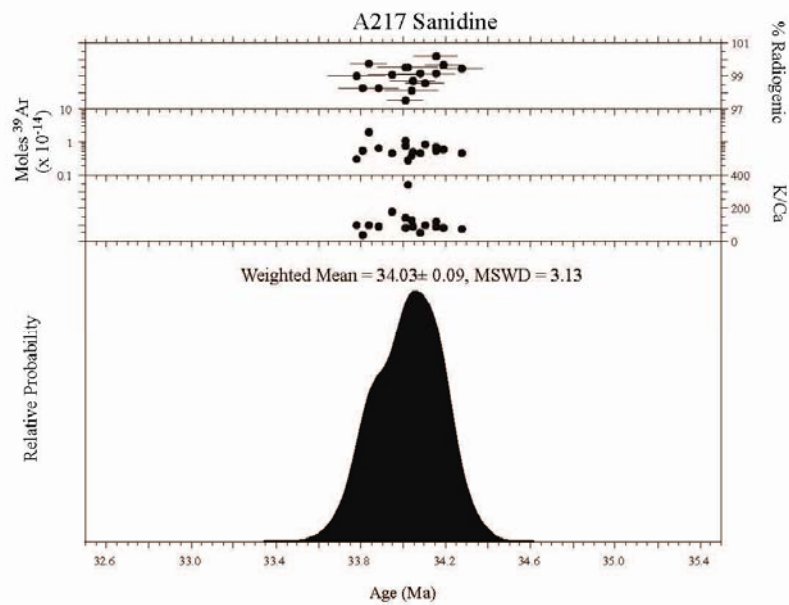


Figure 1. Age probability distribution diagram for A217 sanidine. All errors quoted at 2 Sigma.

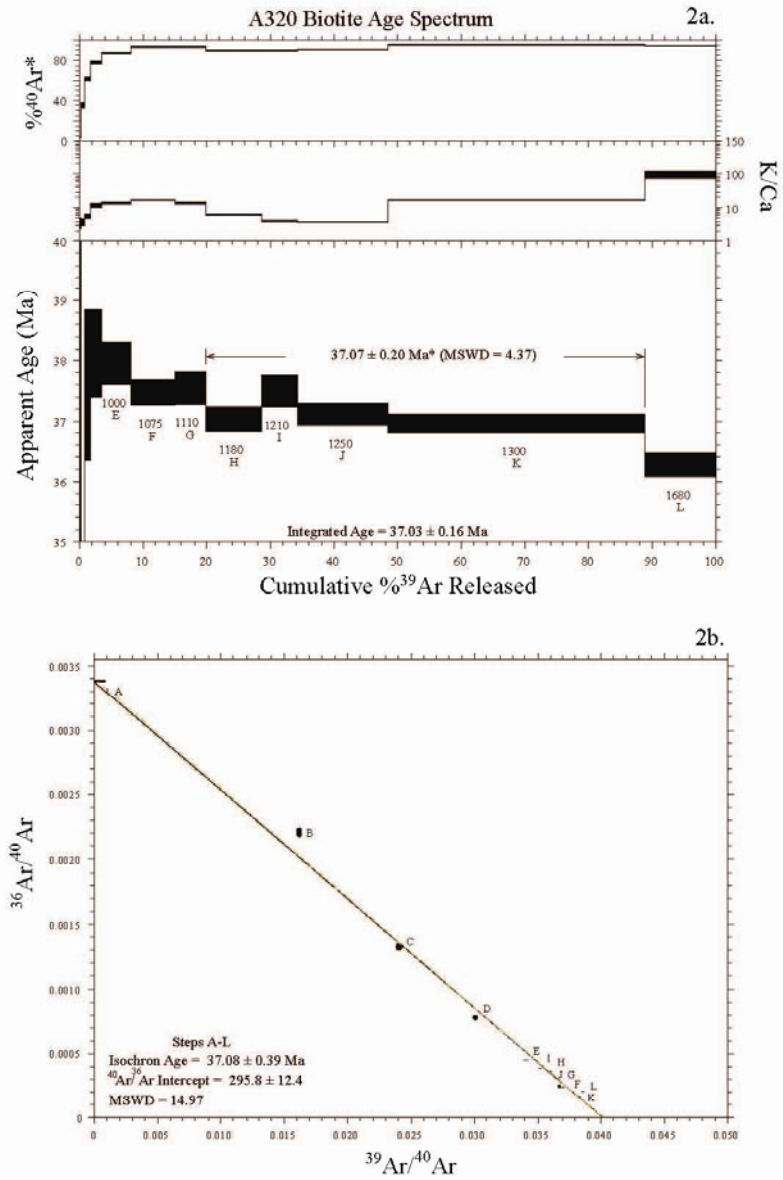


Figure 2. Age spectrum (2a) and isochron (2b) for A320 biotite.
All errors quoted at 2 sigma.

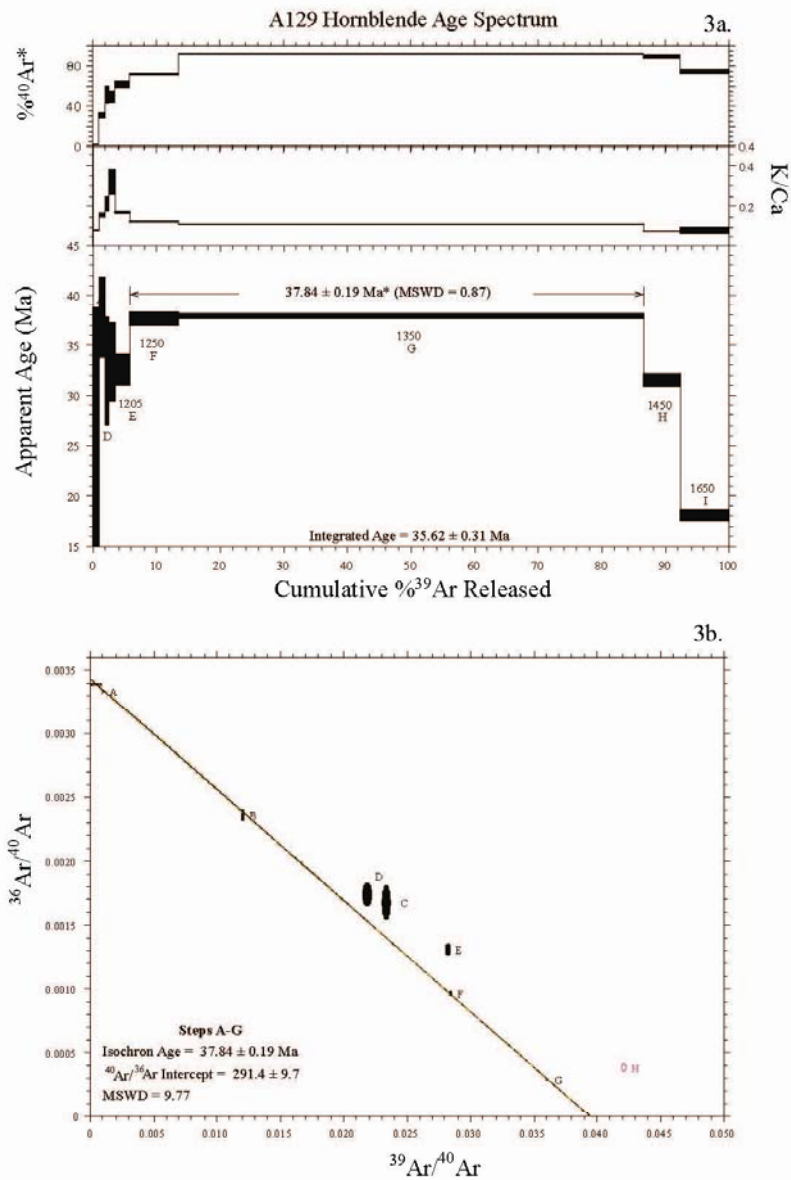


Figure 3. Age spectrum (3a) and isochron (3b) for A129 hornblende.
Point in purple omitted from isochron age calculation.
All errors quoted at 2 sigma.

Table 2. Summary of $^{40}\text{Ar}/^{39}\text{Ar}$ results and analytical methods

Sample	Lab #	Irradiation	mineral	age analysis	steps/analyses	Age	$\pm 2\sigma$	MSWD
A217	58725	NM-221	sanidine	laser total fusion	16	34.03	0.09	3.13
A320	58722	NM-221	biotite	furnace step-heat	4	37.08	0.20	4.37
A129	58723	NM-221	hornblende	furnace step-heat	2	37.84	0.19	0.87

Sample preparation and irradiation:

Minerals separated with standard heavy liquid, Franz Magnetic and hand-picking techniques.

Samples in NM-221 irradiated in a machined Aluminum tray for 7 hours in D-3 position, Nuclear Science Center, College Station, TX.

Neutron flux monitor Fish Canyon Tuff sanidine (FC-2). Assigned age = 28.02 Ma (Renne et al, 1998).

Instrumentation:

Analyses performed on a Mass Analyzer Products 215-50 mass spectrometer on line with automated all-metal extraction system.

Biotite and hornblende step-heated, using a Mo double-vacuum resistance furnace.

Sanidine and flux monitor fused by a 50 watt Synrad CO_2 laser.

Analytical parameters:

Electron multiplier sensitivity averaged 6.88×10^{-17} moles/pA for the biotite analysis, 8.29×10^{-17} moles/pA for the hornblende analysis and 3.35×10^{-17} for the sanidine analysis.

Total system blank and background averaged 1430, 13.3, 5.5, 6.8, 27.4×10^{-18} moles at masses 40, 39, 38, 37 and 36, respectively for the furnace analyses.

Total system blank and background averaged 375, 8.6, 2.2, 2.8, 41.9×10^{-18} moles at masses 40, 39, 38, 37 and 36 for the laser analyses.

J-factors determined by CO_2 laser-fusion of 6 single crystals from each of 10 radial positions around the irradiation tray.

Decay constants and isotopic abundances after Steiger and Jäger (1977).

Table 3. $^{40}\text{Ar}/^{39}\text{Ar}$ analytical data.

ID	$^{40}\text{Ar}/^{39}\text{Ar}$	$^{37}\text{Ar}/^{39}\text{Ar}$	$^{36}\text{Ar}/^{39}\text{Ar}$	$^{39}\text{Ar}_{\text{K}}$	K/Ca	$^{40}\text{Ar}^*$	Age	$\pm 1\sigma$
			($\times 10^{-3}$)	($\times 10^{-15}$ mol)		(%)	(Ma)	(Ma)
A217 , $J=0.0008369\pm0.08\%$, $D=1.0014\pm0.001$, NM-221L, Lab#-58725								
11	22.82	0.0054	0.7967	1.883	93.9	99.0	33.79	0.11
14	23.02	0.0152	1.393	3.279	33.5	98.2	33.81	0.09
02	22.69	0.0057	0.2338	12.337	89.6	99.7	33.84	0.06
08	23.07	0.0062	1.392	3.862	81.7	98.2	33.89	0.07
12	22.92	0.0030	0.7637	2.947	171.5	99.0	33.95	0.10
04	22.85	0.0038	0.3793	4.752	133.5	99.5	34.01	0.07
09	23.32	0.0069	1.974	6.649	74.4	97.5	34.01	0.06
16	22.87	0.0015	0.4156	1.698	340.0	99.5	34.03	0.12
07	23.21	0.0043	1.507	2.465	118.6	98.1	34.05	0.10
05	23.07	0.0060	1.030	3.224	85.3	98.7	34.05	0.09
17	22.99	0.0103	0.6918	2.902	49.5	99.1	34.08	0.09
06	23.15	0.0055	1.182	5.154	93.4	98.5	34.11	0.07
10	22.80	0.0044	-0.1299	3.394	116.0	100.2	34.16	0.08
01	23.05	0.0060	0.7038	4.312	85.3	99.1	34.16	0.07
03	22.94	0.0064	0.2771	3.695	79.5	99.6	34.19	0.07
13	23.06	0.0072	0.4785	2.802	70.6	99.4	34.28	0.08
# 15	34.79	8.170	28.05	0.077	0.062	78.1	40.80	2.07
Mean age $\pm 2\sigma$		n=16	MSWD=3.13		107.3 ± 139.9		34.03	0.09

Notes:

Isotopic ratios corrected for blank, radioactive decay, and mass discrimination, not corrected for interfering reactions.

Errors quoted for individual analyses include analytical error only, without interfering reaction or J uncertainties.

Mean age is weighted mean age of Taylor (1982). Mean age error is weighted error of the mean (Taylor, 1982), multiplied by the root of the MSWD where MSWD>1, and also incorporates uncertainty in J factors and irradiation correction uncertainties.

Decay constants and isotopic abundances after Steiger and Jäger (1977).

symbol preceding sample ID denotes analyses excluded from mean age calculations.

Ages calculated relative to FC-2 Fish Canyon Tuff sanidine interlaboratory standard at 28.02 Ma (Renne et al., 1998)

Decay Constant (Λ_{total}) = $5.543\text{e-}10/\text{a}$

Correction factors:

$$(^{39}\text{Ar}/^{37}\text{Ar})_{\text{Ca}} = 0.00068 \pm 5\text{e-}05$$

$$(^{36}\text{Ar}/^{37}\text{Ar})_{\text{Ca}} = 0.00028 \pm 2\text{e-}05$$

$$(^{39}\text{Ar}/^{39}\text{Ar})_{\text{K}} = 0.0125$$

$$(^{40}\text{Ar}/^{39}\text{Ar})_{\text{K}} = 0 \pm 0.0004$$

Table 4. $^{40}\text{Ar}/^{39}\text{Ar}$ analytical data.

ID	Power	$^{40}\text{Ar}/^{39}\text{Ar}$	$^{37}\text{Ar}/^{39}\text{Ar}$	$^{36}\text{Ar}/^{39}\text{Ar}$	$^{38}\text{Ar}/^{39}\text{Ar}$	K/Ca	$^{40}\text{Ar}^*$	^{39}Ar	Age	$\pm 1\sigma$
	(°C)			($\times 10^{-3}$)	($\times 10^{-15}$ mol)		(%)	(%)	(Ma)	(Ma)
A320, Biotite, 6.24 mg, J=0.0008347±0.07%, D=1.0014±0.001, NM-221L, Lab#58722-01										
X A	650	936.4	0.1454	3095.2	0.239	3.5	2.3	0.3	32.53	7.81
X B	750	61.53	0.1391	135.7	0.363	3.7	34.8	0.7	31.99	1.15
X C	850	41.41	0.0991	54.82	0.79	5.1	60.9	1.5	37.58	0.63
X D	920	33.19	0.0469	25.77	1.24	10.9	77.1	2.9	38.11	0.36
X E	1000	29.31	0.0377	13.01	3.50	13.5	86.9	6.8	37.95	0.18
X F	1075	27.03	0.0314	6.415	5.32	16.2	93.0	12.9	37.46	0.11
X G	1110	27.20	0.0384	6.801	3.66	13.3	92.6	17.1	37.55	0.14
H	1180	27.77	0.0878	9.941	6.7	5.8	89.4	25.1	37.02	0.10
I	1210	28.36	0.1345	10.88	4.21	3.8	88.7	30.3	37.50	0.13
J	1250	27.66	0.1427	9.433	10.8	3.6	90.0	43.9	37.10	0.09
K	1300	26.05	0.0300	4.276	30.5	17.0	95.2	86.9	36.95	0.07
X L	1680	25.90	0.0055	5.312	8.5	93.0	93.9	100.0	36.27	0.10
Integrated age ± 2σ			n=12		75.8	9.0	K2O=5.59%		37.03	0.16
Plateau ± 2σ		steps H-K	n=4	MSWD=4.37	52.272	11.713±12.746		68.9	37.07	0.20
Isochron±2σ		steps A-L	n=12	MSWD=14.97		$^{40}\text{Ar}/^{36}\text{Ar}$ = 295.8±12.4			37.08	0.39
A129, Hornblende, 18.22 mg, J=0.0008362±0.07%, D=1.004±0.001, NM-221L, Lab#58723-01										
X A	900	990.5	6.310	3302.2	0.377	0.081	1.5	1.0	22.94	7.90
X B	1050	82.87	3.247	196.0	0.412	0.16	30.4	2.0	37.73	2.00
X C	1090	42.71	2.448	72.08	0.257	0.21	50.6	2.7	32.36	2.67
X D	1150	45.55	1.595	79.40	0.342	0.32	48.8	3.6	33.25	1.97
X E	1200	35.30	3.009	46.94	0.92	0.17	61.4	5.9	32.48	0.81
F	1250	35.06	4.129	34.97	2.95	0.12	71.5	13.5	37.53	0.34
G	1350	27.64	4.556	9.259	28.6	0.11	91.5	86.7	37.86	0.09
Xi H	1450	23.63	6.437	10.85	2.18	0.079	88.7	92.3	31.47	0.34
Xi I	1650	16.21	6.359	16.13	3.00	0.080	73.8	100.0	18.05	0.26
Integrated age ± 2σ			n=9		39.0	0.11	K2O=0.98%		35.62	0.31
Plateau ± 2σ		steps F-G	n=2	MSWD=0.87	31.527	0.113±0.016		80.8	37.84	0.19
Isochron±2σ		steps A-G	n=7	MSWD=9.77		$^{40}\text{Ar}/^{36}\text{Ar}$ = 291.4±9.7			37.84	0.18

Notes:

Isotopic ratios corrected for blank, radioactive decay, and mass discrimination, not corrected for interfering reactions.
 Errors quoted for individual analyses include analytical error only, without interfering reaction or J uncertainties.
 Integrated age calculated by summing isotopic measurements of all steps.
 Integrated age error calculated by quadratically combining errors of isotopic measurements of all steps.
 Plateau age is inverse-variance-weighted mean of selected steps.
 Plateau age error is inverse-variance-weighted mean error (Taylor, 1982) times root MSWD where MSWD>1.
 Plateau error is weighted error of Taylor (1982).
 Decay constants and isotopic abundances after Steiger and Jäger (1977).
 X symbol preceding sample ID denotes analyses excluded from plateau age calculations.
 Weight percent K₂O calculated from ^{39}Ar signal, sample weight, and instrument sensitivity.
 Ages calculated relative to FC-2 Fish Canyon Tuff sanidine interlaboratory standard at 28.02 Ma (Renne et al., 1998)
 Decay Constant (LambdaK (total)) = 5.543e-10/a
 Correction factors:
 $(^{39}\text{Ar}/^{37}\text{Ar})_{\text{Ca}} = 0.00068 \pm 5\text{e-}05$
 $(^{36}\text{Ar}/^{37}\text{Ar})_{\text{Ca}} = 0.00028 \pm 2\text{e-}05$
 $(^{38}\text{Ar}/^{39}\text{Ar})_{\text{K}} = 0.0125$
 $(^{40}\text{Ar}/^{39}\text{Ar})_{\text{K}} = 0 \pm 0.0004$

New Mexico Bureau of Mines and Mineral Resources

Procedures of the New Mexico Geochronology Research Laboratory

For the Period June 1998 – present

**Matthew Heizler
William C. McIntosh
Richard Esser
Lisa Peters**

$^{40}\text{Ar}/^{39}\text{Ar}$ and K-Ar dating

Often, large bulk samples (either minerals or whole rocks) are required for K-Ar dating and even small amounts of xenocrystic, authigenic, or other non-ideal behavior can lead to inaccuracy. The K-Ar technique is susceptible to sample inhomogeneity as separate aliquots are required for the potassium and argon determinations. The need to determine absolute quantities (i.e. moles of $^{40}\text{Ar}^*$ and ^{40}K) limits the precision of the K-Ar method to approximately 1% and also, the technique provides limited potential to evaluate underlying assumptions. In the $^{40}\text{Ar}/^{39}\text{Ar}$ variant of the K-Ar technique, a sample is irradiated with fast neutrons thereby converting ^{39}K to ^{39}Ar through a (n,p) reaction. Following irradiation, the sample is either fused or incrementally heated and the gas analyzed in the same manner as in the conventional K-Ar procedure, with one exception, no argon spike need be added.

Some of the advantages of the $^{40}\text{Ar}/^{39}\text{Ar}$ method over the conventional K-Ar technique are:

1. A single analysis is conducted on one aliquot of sample thereby reducing the sample size and eliminating sample inhomogeneity.
2. Analytical error incurred in determining absolute abundances is reduced by measuring only isotopic ratios. This also eliminates the need to know the exact weight of the sample.
3. The addition of an argon spike is not necessary.
4. The sample does not need to be completely fused, but rather can be incrementally heated. The $^{40}\text{Ar}/^{39}\text{Ar}$ ratio (age) can be measured for each fraction of argon released and this allows for the generation of an age spectrum.

The age of a sample as determined with the $^{40}\text{Ar}/^{39}\text{Ar}$ method requires comparison of the measured $^{40}\text{Ar}/^{39}\text{Ar}$ ratio with that of a standard of known age. Also, several isotopes of other elements (Ca, K, Cl, Ar) produce argon during the irradiation procedure and must be corrected for. Far more in-depth details of the determination of an apparent age via the $^{40}\text{Ar}/^{39}\text{Ar}$ method are given in Dalrymple et al. (1981) and McDougall and Harrison (1988).

Analytical techniques

Sample Preparation and irradiation details

Mineral separates are obtained in various fashions depending upon the mineral of interest, rock type and grain size. In almost all cases the sample is crushed in a jaw crusher and ground in a disc grinder and then sized. The size fraction used generally corresponds to the largest size possible which will permit obtaining a pure mineral separate. Following sizing, the sample is washed and dried. For plutonic and metamorphic rocks and lavas, crystals are separated using standard heavy liquid, Franz magnetic and hand-picking techniques. For volcanic sanidine and plagioclase, the sized sample is reacted with 15% HF acid to remove glass and/or matrix and then thoroughly washed prior to heavy liquid and magnetic separation. For groundmass concentrates, rock fragments are selected which do not contain any visible phenocrysts.

The NMGRl uses either the Ford reactor at the University of Michigan or the Nuclear Science Center reactor at Texas A&M University. At the Ford reactor, the L67 position is used (unless otherwise noted) and the D-3 position is always used at the Texas A&M reactor. All of the Michigan irradiations are carried out underwater without any shielding for thermal neutrons, whereas the Texas irradiations are in a dry location which is shielded with B and Cd. Depending upon the reactor used, the mineral separates are loaded into either holes drilled into Al discs or into 6 mm I.D. quartz tubes. Various Al discs are used. For Michigan, either six hole or twelve hole, 1 cm diameter discs are used and all holes are of equal size. Samples are placed in the 0, 120 and 240° locations and standards in the 60, 180 and 300° locations for the six hole disc. For the twelve hole disc, samples are located at 30, 60, 120, 150, 210, 240, 300, and 330° and standards at 0, 90, 180 and 270 degrees. If samples are loaded into the quartz tubes, they are wrapped in Cu foil with standards interleaved at ~0.5 cm intervals. For Texas, 2.4 cm diameter discs contain either sixteen or six sample holes with smaller holes used to hold the standards. For the six hole disc, sample locations are 30, 90, 150, 210, 270 and 330° and standards are at 0, 60, 120, 180, 240 and 300°. Samples are located at 18, 36, 54, 72, 108, 126, 144, 162, 198, 216, 234, 252, 288, 306, 324, 342 degrees and standards at 0, 90, 180 and 270 degrees in the sixteen hole disc. Following sample loading into the discs, the discs are stacked, screwed together and sealed

in vacuo in either quartz (Michigan) or Pyrex (Texas) tubes.

Extraction Line and Mass Spectrometer details

The NMGRL argon extraction line has both a double vacuum Mo resistance furnace and a CO₂ laser to heat samples. The Mo furnace crucible is heated with a W heating element and the temperature is monitored with a W-Re thermocouple placed in a hole drilled into the bottom of the crucible. A one inch long Mo liner is placed in the bottom of the crucible to collect the melted samples. The furnace temperature is calibrated by either/or melting Cu foil or with an additional thermocouple inserted in the top of the furnace down to the liner. The CO₂ laser is a Synrad 10W laser equipped with a He-Ne pointing laser. The laser chamber is constructed from a 3 3/8" stainless steel conflat and the window material is ZnS. The extraction line is a two stage design. The first stage is equipped with a SAES GP-50 getter, whereas the second stage houses two SAES GP-50 getters and a tungsten filament. The first stage getter is operated at 450°C as is one of the second stage getters. The other second stage getter is operated at room temperature and the tungsten filament is operated at ~2000°C. Gases evolved from samples heated in the furnace are reacted with the first stage getter during heating. Following heating, the gas is expanded into the second stage for two minutes and then isolated from the first stage. During second stage cleaning, the first stage and furnace are pumped out. After gettering in the second stage, the gas is expanded into the mass spectrometer. Gases evolved from samples heated in the laser are expanded through a cold finger operated at -140°C and directly into the second stage. Following cleanup, the gas in the second stage and laser chamber is expanded into the mass spectrometer for analysis.

The NMGRL employs a MAP-215-50 mass spectrometer which is operated in static mode. The mass spectrometer is operated with a resolution ranging between 450 to 600 at mass 40 and isotopes are detected on a Johnston electron multiplier operated at ~2.1 kV with an overall gain of about 10,000 over the Faraday collector. Final isotopic intensities are determined by linear regression to time zero of the peak height versus time following gas introduction for each mass. Each mass intensity is corrected for mass spectrometer baseline and background and the extraction system blank.

Blanks for the furnace are generally determined at the beginning of a run while the furnace is cold and then between heating steps while the furnace is cooling. Typically, a blank is

run every three to six heating steps. Periodic furnace hot blank analysis reveals that the cold blank is equivalent to the hot blank for temperatures less than about 1300°C. Laser system blanks are generally determined between every four analyses. Mass discrimination is measured using atmospheric argon which has been dried using a Ti-sublimation pump. Typically, 10 to 15 replicate air analyses are measured to determine a mean mass discrimination value. Air pipette analyses are generally conducted 2-3 times per month, but more often when samples sensitive to the mass discrimination value are analyzed. Correction factors for interfering nuclear reactions on K and Ca are determined using K-glass and CaF₂, respectively. Typically, 3-5 individual pieces of the salt or glass are fused with the CO₂ laser and the correction factors are calculated from the weighted mean of the individual determinations.

Data acquisition, presentation and age calculation

Samples are either step-heated or fused in a single increment (total fusion). Bulk samples are often step-heated and the data are generally displayed on an age spectrum or isochron diagram. Single crystals are often analyzed by the total fusion method and the results are typically displayed on probability distribution diagrams or isochron diagrams.

The Age Spectrum Diagram

Age spectra plot apparent age of each incrementally heated gas fraction versus the cumulative % ³⁹Ar_K released, with steps increasing in temperature from left to right. Each apparent age is calculated assuming that the trapped argon (argon not produced by *in situ* decay of ⁴⁰K) has the modern day atmospheric ⁴⁰Ar/³⁶Ar value of 295.5. Additional parameters for each heating step are often plotted versus the cumulative %³⁹Ar_K released. These auxiliary parameters can aid age spectra interpretation and may include radiogenic yield (percent of ⁴⁰Ar which is not atmospheric), K/Ca (determined from measured Ca-derived ³⁷Ar and K-derived ³⁹Ar) and/or K/Cl (determined from measured Cl-derived ³⁸Ar and K-derived ³⁹Ar). Incremental heating analysis is often effective at revealing complex argon systematics related to excess argon, alteration, contamination, ³⁹Ar recoil, argon loss, etc. Often low-temperature heating steps have low radiogenic yields and apparent ages with relatively high errors due mainly to

loosely held, non-radiogenic argon residing on grain surfaces or along grain boundaries. An entirely or partially flat spectrum, in which apparent ages are the same within analytical error, may indicate that the sample is homogeneous with respect to K and Ar and has had a simple thermal and geological history. A drawback to the age spectrum technique is encountered when hydrous minerals such as micas and amphiboles are analyzed. These minerals are not stable in the ultra-high vacuum extraction system and thus step-heating can homogenize important details of the true ^{40}Ar distribution. In other words, a flat age spectrum may result even if a hydrous sample has a complex argon distribution.

The Isochron Diagram

Argon data can be plotted on isotope correlation diagrams to help assess the isotopic composition of Ar trapped at the time of argon closure, thereby testing the assumption that trapped argon isotopes have the composition of modern atmosphere which is implicit in age spectra. To construct an “inverse isochron” the $^{36}\text{Ar}/^{40}\text{Ar}$ ratio is plotted versus the $^{39}\text{Ar}/^{40}\text{Ar}$ ratio. A best fit line can be calculated for the data array which yields the value for the trapped argon (Y-axis intercept) and the $^{40}\text{Ar}^*/^{39}\text{Ar}_K$ value (age) from the X-axis intercept. Isochron analysis is most useful for step-heated or total fusion data which have a significant spread in radiogenic yield. For young or low K samples, the calculated apparent age can be very sensitive to the composition of the trapped argon and therefore isochron analysis should be performed routinely on these samples (cf. Heizler and Harrison, 1988). For very old (>Mesozoic) samples or relatively old sanidines (>mid-Cenozoic) the data are often highly radiogenic and cluster near the X-axis thereby making isochron analysis of little value.

The Probability Distribution Diagram

The probability distribution diagram, which is sometimes referred to as an ideogram, is a plot of apparent age versus the summation of the normal distribution of each individual analysis (Deino and Potts, 1992). This diagram is most effective at displaying single crystal laser fusion data to assess the distribution of the population. The K/Ca, radiogenic yield, and the moles of ^{39}Ar for each analysis are also often displayed for each sample as this allows for visual ease in identifying apparent age correlations between, for instance, plagioclase contamination, signal size and/or radiogenic concentrations. The error (1σ) for each age analysis is generally shown by the horizontal lines in the moles of ^{39}Ar section. Solid symbols represent the analyses used for the weighted mean age calculation and the generation of the solid line on the ideogram, whereas open symbols represent data omitted from the age calculation. If shown, a dashed line represents the probability distribution of all of the displayed data. The diagram is most effective for displaying the form of the age distribution (i.e. gaussian, skewed, etc.) and for identifying xenocrystic or other grains which fall outside of the main population.

Error Calculations

For step-heated samples, a plateau for the age spectrum is defined by the steps indicated. The plateau age is calculated by weighting each step on the plateau by the inverse of the variance and the error is calculated by either the method of Samson and Alexander (1987) or Taylor (1982). A mean sum weighted deviates (MSWD) value is determined by dividing the Chi-squared value by $n-1$ degrees of freedom for the plateau ages. If the MSWD value is outside the 95% confidence window (cf. Mahon, 1996; Table 1), the plateau or preferred age error is multiplied by the square root of the MSWD.

For single crystal fusion data, a weighted mean is calculated using the inverse of the variance to weight each age determination (Taylor, 1982). Errors are calculated as described for the plateau ages above.

Isochron ages, $^{40}\text{Ar}/^{36}\text{Ar}_i$ values and MSWD values are calculated from the regression results obtained by the York (1969) method.

References cited

- Dalrymple, G.B., Alexander, E.C., Jr., Lanphere, M.A., and Kraker, G.P., 1981. Irradiation of samples for $^{40}\text{Ar}/^{39}\text{Ar}$ dating using the Geological Survey TRIGA reactor. U.S.G.S., Prof. Paper, 1176.
- Deino, A., and Potts, R., 1990. Single-Crystal $^{40}\text{Ar}/^{39}\text{Ar}$ dating of the Olorgesailie Formation, Southern Kenya Rift, J. Geophys. Res., 95, 8453-8470.
- Deino, A., and Potts, R., 1992. Age-probability spectra from examination of single-crystal $^{40}\text{Ar}/^{39}\text{Ar}$ dating results: Examples from Olorgesailie, Southern Kenya Rift, Quat. International, 13/14, 47-53.
- Fleck, R.J., Sutter, J.F., and Elliot, D.H., 1977. Interpretation of discordant $^{40}\text{Ar}/^{39}\text{Ar}$ age-spectra of Mesozoic tholeiites from Antarctica, Geochim. Cosmochim. Acta, 41, 15-32.
- Heizler, M. T., and Harrison, T. M., 1988. Multiple trapped argon components revealed by $^{40}\text{Ar}/^{39}\text{Ar}$ analysis, Geochim. Cosmochim. Acta, 52, 295-1303.
- Mahon, K.I., 1996. The New "York" regression: Application of an improved statistical method to geochemistry, International Geology Review, 38, 293-303.
- McDougall, I., and Harrison, T.M., 1988. Geochronology and thermochronology by the ^{40}Ar - ^{39}Ar method. Oxford University Press.
- Samson, S.D., and, Alexander, E.C., Jr., 1987. Calibration of the interlaboratory $^{40}\text{Ar}/^{39}\text{Ar}$ dating standard, Mmhb-1, Chem. Geol., 66, 27-34.
- Steiger, R.H., and Jäger, E., 1977. Subcommission on geochronology: Convention on the use of decay constants in geo- and cosmochronology. Earth and Planet. Sci. Lett., 36, 359-362.
- Taylor, J.R., 1982. An Introduction to Error Analysis: The Study of Uncertainties in Physical Measurements., Univ. Sci. Books, Mill Valley, Calif., 270 p.
- York, D., 1969. Least squares fitting of a straight line with correlated errors, Earth and Planet. Sci. Lett., 5, 320-324.